The Synthesis and Study of Redox-Rich, Amido-Bridged Cu_2N_2 Dicopper Complexes

Thesis by

Seth Beebe Harkins

In Partial Fulfillment of the Requirements

for the Degree of Doctor of Philosophy

California Institute of Technology

Pasadena, California

2006

(Defended June 27, 2005)

Acknowledgment

First and foremost, I must thank my parents and family, for they have taught me more life lessons than I can count and have given me unconditional love and support. In particular, I thank my father for teaching me the life lesson that "A job worth doing, is a job worth doing right." As trite as it may seem, it is a lesson that has transcended to my chemical endeavors and has encouraged excellence in my scientific pursuits. To my mother, my first instructor in the chemical sciences, I thank you for your candor and insistence that no matter what you do in life, to make sure that it is what makes you most happy. With this paradigm in mind, it is my pleasure to state that I am still elated every day I have the opportunity to walk into the laboratory and make something new.

I thank Professor Ayusman Sen for giving me the opportunity to work in his lab as an undergraduate. It was this chance to be involved with chemistry at the forefront of innovation that made it clear to me that inorganic chemistry was to be my field of choice. I thank him for encouraging me, in the face of adversity, to purse graduate study at the very best institution possible. From the Sen Lab, I would also like to thank then graduate students, Dr. Jim Pawlow, Dr. Shahid Murtuza, and Dr. April D. Hennis Marchetti, for putting up with me as an eager undergraduate researcher and always helping me in spite of the sacrifice to their own productivity. I would also like to acknowledge John D. Higgins, III for being a role model to me in what I wanted from my life as a synthetic chemist. I have never met anyone who made it so cool to be a nerd as John.

I wish to acknowledge my fellow "idiot troops" in the Peters Lab for adding levity to the research environment, happily serving as a sounding board for my chemical ramblings, and providing lots of well-needed proofreading. In particular, I would like to

thank the irreplaceable combination of Dr. Steven D. Brown and Dr. Theodore A. Betley for many a diversion from work, endless reality checks, and their essential thoughts on chemistry. I have also really appreciated my box-mate, Dr. Cora E. MacBeth, for constant conversation, input on my project, "decorating" the ceiling of the dry-box, and not getting too irritated with me when I destroy the atmosphere with methylene chloride.

With the uttermost sincerity, I express my gratitude to my adviser Professor Jonas C. Peters for giving me the latitude to always chase my ideas, even when he didn't quite know why I was doing it at the time. He had the foresight to create a near perfect laboratory environment for inorganic synthesis and then to stock it with a unique blend of graduate students and post-docs that produced science worthy of his tenure. I am happy to have been part of the legacy. Moreover (that one is for you Jonas), I would like to thank my committee, Professors John D. Bercaw, Harry B. Gray, and David A. Tirrell for critical evaluation and suggestions for my project, as well as thoughtful discussions of my propositions. I would like to acknowledge the Institute, the Division of Chemistry and Chemical Engineering, and the supporting cast of faculty, scientists, and staff members, which is not limited to Bruce Brunschwig, Michael Day, Angelo Di Bilio, Dian Buchness, Rick Gerhart, Kathleen Hand, Larry Henling, Jay R. Winkler, and the members of the Gray and Bercaw research groups.

Finally, I thank my loving wife Jennifer for giving me a reason to go home every night. You are the love of my life and you have made me a better person and a better scientist over the past five years. I also thank you for your tireless assistance with the numerous laser experiments presented herein; without you they would not have been possible. I look forward to starting the next stage of my life with you.

Abstract

A Cu_2N_2 diamond core structure supported by an $[SNS]^-$ ligand exhibits a fully reversible one-electron redox process between a reduced Cu^ICu^I, $\{(SNS)Cu\}_2$, and a class III delocalized $Cu^{1.5}Cu^{1.5}$ state, $[\{(SNS)Cu\}_2][B(C_6H_3(CF_3)_2)_4]$ ($[SNS]^-$ = bis(2-*t*-butylsulfanylphenyl)amide). The Cu···Cu distance compresses appreciably (~0.13 Å) upon oxidation; a metal-metal distance of 2.4724(4) Å is observed in the mixed-valence molecule that is nearly identical to the dicopper Cu_A site found in cytochrome *c* oxidase. The rate of electron self-exchange (k_s) between the Cu^ICu^I and the $Cu^{1.5}Cu^{1.5}$ complexes was estimated to be $\geq 10^7$ $M^{-1}s^{-1}$ by ^1H NMR line-broadening analysis. The unusually large magnitude of k_s reflects the minimal structural reorganization that accompanies $Cu^ICu^I \leftrightarrow Cu^{1.5}Cu^{1.5}$ interchange.

A second generation of $\{(PNP)Cu^I\}_2$ dimer supported by a $[PNP]^-$ ligand also has been investigated ($[PNP]^-$ = bis(2-(diisobutylphosphino)phenyl)amide). The highly emissive $\{(PNP)Cu^I\}_2$ is characterized by a long-lived excited state ($\tau > 10$ μs) with an unusually high quantum yield ($\phi > 0.65$) at ambient temperature. Removal of an electron from the $\{(PNP)Cu^I\}_2$ dimer yields a nearly isostructural, $Cu^{1.5}Cu^{1.5}$ complex $[\{(PNP)Cu\}_2][B(C_6H_3(CF_3)_2)_4]$. With a highly reducing excited state reduction potential (~ −3.2 V vs. Fc^+/Fc) as well as the availability of two reversible redox processes, these bimetallic copper systems may be interesting candidates for photochemically driven two-electron redox transformations.

Studies of Cu_2N_2 diamond core complexes supported by the $[^tBu_2\text{-}PNP]^-$ ligand revealed that the dicopper complex $\{(^tBu_2\text{-}PNP)Cu\}_2$ can not only be oxidized by one electron to $[\{(^tBu_2\text{-}PNP)Cu^{1.5}\}_2][B(C_6H_3(CF_3)_2)_4]$, but also by two-electrons to [{(tBu2-

PNP)Cu}$_2$][SbF_6]$_2$ ([^{t}Bu$_2$-PNP]$^-$ = bis(2-diisobutylphoshino-4-^{t}butylphenyl)amide). These Cu_2N_2 complexes show remarkably low structural reorganization for all oxidation states as evidenced by the solid-state molecular-structures. Based on these studies of [{(^{t}Bu$_2$-PNP)Cu}$_2$][SbF_6]$_2$, we propose a formulation of one Cu^I and one paramagnetic Cu^{III} nuclei in compressed-tetrahedral environments in the Cu_2N_2 core. Spectroscopic, redox, and magnetic data are consistent with a highly covalent M_2N_2 core supported by a rigid ligand scaffold. These complexes are excellent mimics of the entatic state found in bimetallic copper proteins.

Table of Contents

List of Figures, Graphs, and Tables

Chapter I

Chapter II

Chapter III

Chapter IV

Appendix A

Nomenclature

$\{^{1}H\}$	hydrogen-1 decoupled
°	degrees in measure of angles
°C	degrees Celsius
^{1}H	hydrogen-1
^{13}C	carbon-13
^{19}F	fluorine-19
^{31}P	phosphorus-31
Å	Angstrom, 10^{-10} m
Anal. Calcd	elemental analysis calculated
Ar	general aryl group
av	average
A_x	EPR hyperfine coupling where X is the nucleus coupling to the unpaired electron (also sometimes abbreviated A_x)
BAr^F	tetrakis(3,5-trifluoromethylphenyl)borate
B3LYP	Becke three-parameter functional with Lee-Yang-Parr correlation functional
BM	Bohr magnetons
br	broad
BQA	bis(8-quinolinyl)amido
Bu	butyl
Calcd	calculated
CCD	charge coupled device

cm	centimeter(s)
cm^{-1}	inverse centimeters or wavenumbers
cm^{3}	cubic centimeters
cont.	continued
d	doublet
DC	direct current
deg	degrees in measure of angles
DFT	density functional theory
E	an atom or functional group forming a metal-ligand multiple bond EPR electron paramagnetic resonance
Eq.	equation
equiv.	equivalents
ESI/MS	electrospray ionization mass spectrometry
Et	ethyl
fac	facial coordination
g	gram
G	gauss
GC/MS	gas chromatography mass spectrometry
GHz	gigahertz
g_{iso}	isotropic g-factor
h	hour(s)
H	applied magnetic field
HOMO	highest occupied molecular orbital

Hz	hertz
I_n	nuclear spin of atom n
^{i}Pr	iso-propyl
IR	infrared
K	degrees in Kelvin
Kcal	kilocalories
kHz	kilohertz
L	dative ligand for a transition metal
LACVP	Los Alamos core valence potential
LFT	ligand field theory
LUMO	lowest unoccupied molecular orbital
m	multiplet
M	general metal
Me	methyl
Mes	mesityl
mg	milligram(s)
MHz	megahertz, one million Hertz
min	minute(s)
mL	milliliter(s)
mmol	millimoles
MO	molecular orbital
mol	moles
ms	millisecond(s)

MS	mass spectrometry
mT	millitesla(s)
mV	millivolt(s)
mW	milliwatt(s)
NA	not applicable
^{n}Bu	n-butyl
near-IR	near-infrared
nm	namometer(s)
NMR	nuclear magnetic resonance
OTf	trifluoromethanesoulphonate
p-	para position on an aryl ring
Ph	phenyl
PMe_3	trimethyl phosphine
PNP	bis(2-(diisobutylphosphino)phenyl)amide
$^{t}Bu_2$-PNP	bis(2-diisobutylphoshino-4-^{t}butylphenyl)amide
ppm	parts per million
q	quartet
R	general alkyl or aryl substituent
s	second(s)
S	spin
SNS	bis(2-tertbutylsulfanylphenyl)amide
SOMO	singly occupied molecular orbital
SQUID	superconducting quantum interference device

T	temperature
TBA	tetrabutylammonium
^{t}Bu	tert-butyl
THF	tetrahydrofuran
TMS	trimethylsilyl
UV-vis	ultraviolet-visible
X	monoanionic atom or group, such as a halide or thiolate
XRD	X-ray diffraction
δ	delta, chemical shift
ε	extinction coefficient in M^{-1} cm^{-1}
λ	wavelength
λ_{max}	wavelength of maximum absorption
μ	absorption coefficient (X-ray diffraction)
μ-A	bridging atom
μ_B	Bohr magnetons
μ_{eff}	effective magnetic moment, measured in Bohr magnetons
μL	microliter(s)
ν	frequency
θ	Weiss constant
χ	magnetic susceptibility
χ_m	molar magnetic susceptibility

Chapter I

Late Transition Metal Complexes of Chelating Amido Ligands[†]

[†] Text taken in part from Peters, J. C.; Harkins, S. B.; Brown, S. D.; Day, M. W. *Inorg. Chem.* **2001**, *40*, 5083. Harkins, S. B.; Peters, J. C. *Organometallics* **2002**, *21*, 1753. Harkins, S. B.; Peters, J. C. *J. Am. Chem. Soc.* **2004**, *126*, 2885. Harkins, S. B.; Peters, J. C. *J. Am. Chem. Soc.* **2005**, *127*, 2030.

I.A. Thesis Overview and Motivation

Here is presented the first preparation of amido-bridged Cu_2N_2 dicopper coordination complexes and the subsequent study of their rich spectroscopic and redox properties. These unique metal dimers are supported by chelating diaryl amido ligands that give rise to M_2N_2 diamond core configurations with overall D_2 symmetry (Figure I.1). As a result of this thesis work, we have demonstrated that these ligand scaffolds allow for the metal centers to reside in a protein like "entatic state," which facilitates low structural reorganization upon oxidation or photoexcitation of the $d^{10}d^{10}$ metal complexes. Vallee and Williams have described the entatic state as the constrained environment of an enzymatic active site which allows for specific activity, while minimizing the reorganization energy needed to reach the transition state.[1] This characteristic gives rise to a multitude of interesting consequences which include rapid inter- and intra-molecular electron transfer phenomena, intense photoluminescence, and stability in multiple oxidation states. All of these processes occur without changes to the coordination number or structural distortion of the overall molecule. As a whole, these advances have added a new dimension to the field of dicopper chemistry and laid the ground work for many further studies in the general area of late transition metal chemistry supported by amide ligands.

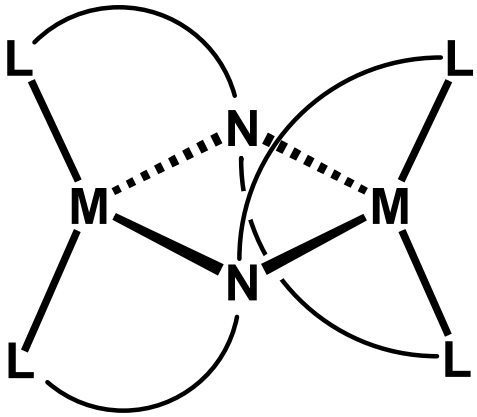

Figure I.1. Generalized M_2N_2 diamond-core complex. {M = Li, Cu, Zn; L = N, O, P, S}.

Dicopper electron transfer (ET) cofactors in biology are now well established, yet the topic of how the site is able to minimize structural reorganization and maintain its coordination geometry during this process is still of interest.[2,3,4] For example, a collection of spectroscopic and, more recently, structural data has revealed that cytochrome *c* oxidase accomplishes enhanced ET rates into and out of a buried Cu_A site by virtue of a highly covalent, thiolate-bridged Cu_2S_2 diamond-core structure (Figure I.2).[5,6,7]

Amongst the various low molecular weight systems that have been developed to model aspects of this Cu_A site,[8,9,10,11] perhaps the most structurally relevant to the enzyme is Tolman's thiolate-bridged, mixed-valence $\{L^{N3S}Cu^{1.5}\}_2^+$ diamond-core complex.[8a] This complex features an EPR signal consistent with a fully-delocalized, class III, diamond- core description,[5b,8a] as is observed for the resting state form of the Cu_A site.[5b,6] Despite this similarity, the Cu···Cu distance in the Tolman model system is much larger than that observed in Cu_A, and the complex does not reproduce the reversible Cu^ICu^I to $Cu^{1.5}Cu^{1.5}$ redox behavior observed for the enzyme. Several dicopper systems that diverge from the diamond core structural motif do show reversible redox behavior for a $Cu^{1.5}Cu^{1.5}$ mixed-valence state.[10c,12] For example, a family of dicopper azacryptates that successfully bring the two copper centers into much closer proximity (~ 2.35–2.4Å) has been developed,[12a] and many of these can undergo rapid electron self-exchange (k_s) between their oxidized and reduced forms (~ 10^5 M^{-1} s^{-1}).[12b]

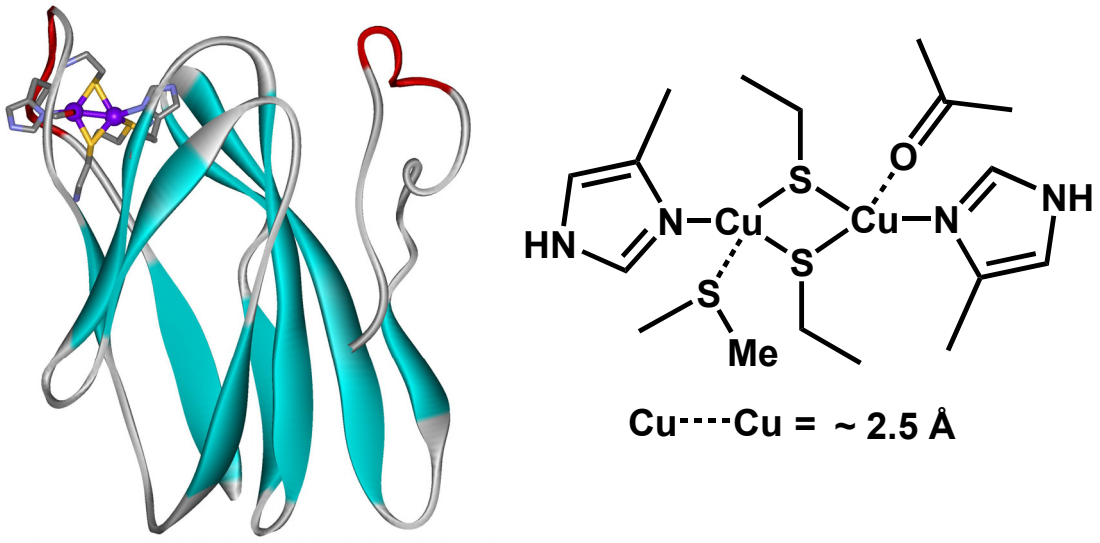

Figure I.2. *Left,* Schematic of cytochrome *c* oxidase from *Thermus thermophilius* ba_3;[7] *right*, Core representation of the Cu_A site.

Diamond core copper systems that reversibly model *both* the reduced Cu^ICu^I and the delocalized $Cu^{1.5}Cu^{1.5}$ redox states observed in Cu_A had yet to be developed.[13] Ligand systems that would help to minimize structural reorganization between these two redox forms and hold the two copper centers of a diamond core in close enough proximity to reproduce the short Cu-Cu bond distance observed in Cu_A (~2.5 Å)[14] might serve as simplified functional models for the redox behavior of Cu_A.[5b,c,d] One avenue into this regime using small molecule design is to replace the thiolate bridging units inherent to the Cu_2S_2 diamond core of Cu_A with amido bridging units. Such a strategy should slide the copper centers closer together so as to better model the distance observed in Cu_A while still maintaining a Cu_2X_2 diamond core motif. Moreover, it was thought that such an approach might shed some light on whether the thiolate moiety plays a unique role in facilitating rapid electron transfer chemistry by bringing the two copper centers of a diamond core into strong electronic communication.

In Chapter II, this topic has been addressed through the synthesis and study of a Cu_2N_2 diamond core system supported by the tridentate amido ligand, bis(2-tertbutylsulfanylphenyl)amido (Figure II.3). These dicopper systems were found to exhibit a fully reversible and very facile one electron redox process between a Cu^1Cu^1 and a class III delocalized $Cu^{1.5}Cu^{1.5}$ form. Solid-state structural snapshots of both redox forms reveal (i) very short Cu···Cu distances akin to those in Cu_A, and (ii) minimal structural reorganization upon oxidation from the reduced Cu^1Cu^1 to the delocalized $Cu^{1.5}Cu^{1.5}$ state. These features facilitate very facile rates of electron self-exchange between the reduced and one electron oxidized forms of the system ($\geq 10^7$ M^{-1} s^{-1}). To our knowledge, this is the fastest electron self-exchange rate reported for low molecular weight copper complexes.[3a,12b] A distinct Cu···Cu compression accompanies the one electron oxidation process and may reflect the onset of direct Cu-Cu electronic exchange. Using cyclic voltammetry, this reversible one electron oxidation was found to occur at -250 mV vs. Fc^+/Fc in THF. A marginally-reversible wave at higher potential ($E_{pa} \approx +570$ mV), was also observed. We speculated this is an unstable dicopper(II,II) species.

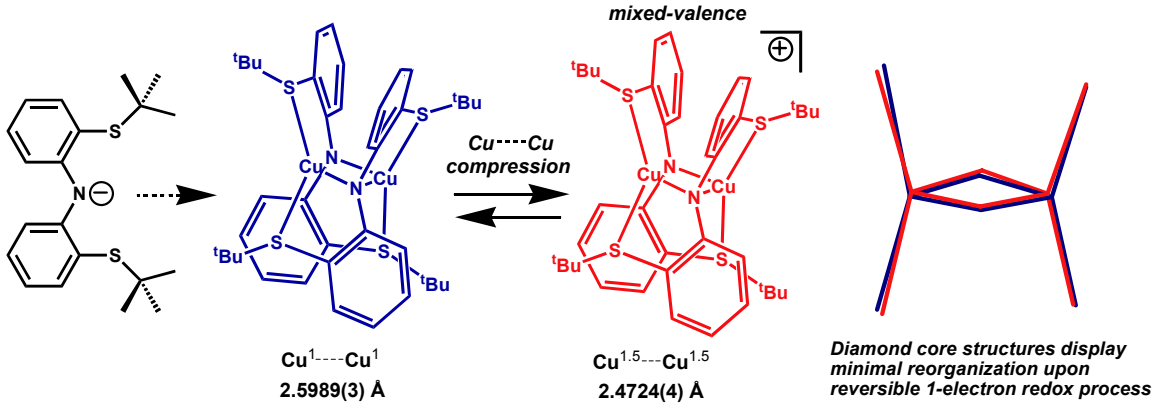

Figure I.3. Schematic summary of Cu_2N_2 core contraction upon oxidation.

Optimistic at the possibility of obtaining a system that could mediate two sequential one-electron oxidations with nominal change to the coordination sphere, we began to explore the effects of ligand modification. It was conjectured that by switching from thioether to more reducing alkyl phosphine chelates, an electron-rich Cu_2N_2 complexes would result. By shifting the dicopper redox potential more negative, it was thought that perhaps both oxidation processes would be stabilized. This was accomplished by using bis(2-diisobutylphosphinophenyl)amido, $[PNP]^-$, ligands. Similar Cu_2N_2 complexes were afforded (Figure I.4) with this new ligand and now two reversible one electron processes were observed by cyclic voltammetry. Surprisingly, we found that $\{(PNP)Cu\}_2$ complex was an exceptional luminophore (Figure I.4). The photophysical properties of this complex are the topic of Chapter III. Notably, $\{(PNP)Cu^I\}_2$ is characterized by a long-lived excited state (τ > 10 μs) with an unusually high quantum yield (ϕ > 0.65) at ambient temperature.

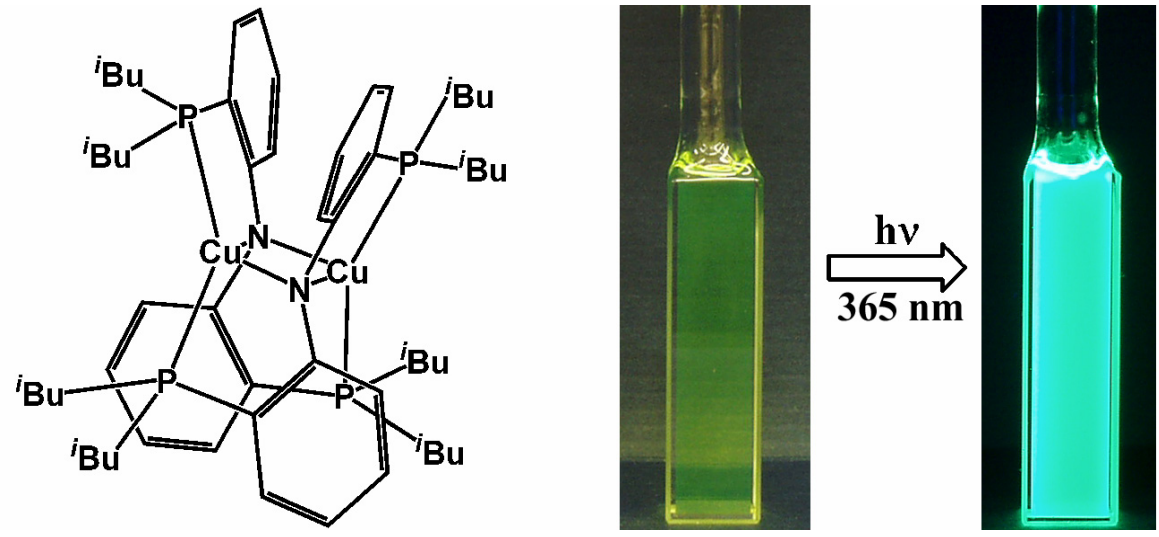

Figure I.4. *Left*, Schematic representation of $\{(PNP)Cu^I\}_2$; *right*, Photo of $\{(PNP)Cu^I\}_2$ in petroleum ether solution in room light and upon irradiation with 365 nm light.

Photoluminescent polypyridine-supported Cu^I systems have garnered much attention due to their promise as low cost organic light emitting devices.[15] However, the tendency of Cu^I complexes to display weak emission and short-lived excited states is problematic.[16] McMillin has described these weaknesses in the current systems,[17] and his group recently reported a mononuclear complex, $[Cu(dmp)(POP)]^+$ (dmp = 2,9-dimethyl-1,10-phenanthroline; POP = bis[2-(diphenylphosphino)phenyl]ether)]), that exhibits both a relatively high quantum yield and a long-lived excited-state as compared to other polypyridine-Cu(I) systems.[18] Incorporation of a bulky, bis(phosphine) chelate appears to create a rigid environment around the copper center which (i) suppresses solvent-induced exciplex formation, and (ii) limits problematic ligand dissociation from the excited state. It is likely that through the same property of low structural reorganization energy that gives rise to rapid electron transfer between the oxidized and reduced forms of the $\{(SNS)Cu\}_2$ system, highly conserved photon emission is now observed. We have found these PNP supported Cu dimers are among the most emissive inorganic complexes that have been reported and postulate that the intense emission may result from a direct Cu↔Cu interaction.

Returning to the redox chemistry of the Cu_2N_2 species, the chemical oxidation of $\{(PNP)Cu^I\}_2$ was evaluated with the intention of developing photolytically driven two-electron chemistry. Chapter IV details the multielectron redox processes of the PNP dicopper complexes. Through targeted ligand modification, dicopper complexes in three oxidation states with pseudo-tetrahedral geometries are described in terms of their solid-state molecular structures, spectral and magnetic properties. The preparations of the isoelectronic dizinc and mixed copper-zinc dimers are also discussed. These latter

complexes serve to highlight the unique character of the Cu↔Cu interaction to function of the system. Based on our studies, it is evident that much of this stabilization results from delocalization across the entire molecular scaffold.

I.B. Summary of Group 10 metal studies

Our initial work in the exploration of late transition metal amide chemistry focused on the Group 10 transition metals. In order to build new molecular systems relevant to our goals of exploring small-molecule activation and uncovering novel metal-ligand coordination environments, robust anionic chelating ligands were pursued. Initially complexes based on the monoanionic chelating ligand bis(8-quinolinyl)amine, (BQA)H, and its structural analogues were targeted. The synthesis of (BQA)H had been first reported by Nielsen in 1964,[19] and the first reported metallation followed in 1986, when Petersen published the crystal structure of the square planar complex,[20] $(BQA)Cu^{II}Cl$. The literature preparation of (BQA)H was achieved by condensation of 8-hydroxyquinoline and 8-aminoquinoline in a Bucherer-type reaction.[7,8] Yields were of less than 10% after one week of reflux which was unacceptable for producing multi-gram quantities of the ligand. Thus, a catalytic cross-coupling strategy was targeted.[21] Pd-coupling of commercially available 8-aminoquinoline and 8-bromoquinoline was achieved under typical reaction conditions ($Pd_2(dba)_3$, toluene, 110 °C, 3 days) with NaO^tBu as the base and rac-BINAP as the cocatalyst.[22] Recrystallization of the crude product afforded orange crystalline solid, typically in yields in excess of 85%.

This strategy enabled the generation of a readily prepared family of useful, monoanionic amido ligands, Figure I.5. Although hard amido ligands can lead to undesirable reduction and/or degradation of late metal complexes, the use of chelating

amido ligands has been shown to circumvent such problems.[23] Our desire to explore the divalent Group 10 chemistry of (BQA)H was motivated, in part, by the following rationale: Square planar, monoalkyl complexes of ligand (BQA)H should adopt a coordination geometry in which the alkyl group is forced to occupy a coordination site *trans* to the amido nitrogen donor group. Typically, divalent group 9 and 10 complexes containing two strongly *trans*-influencing ligands adopt coordination geometries that place these two ligands *cis* to one another.[24] The BQA ligand discriminates against such a *cis* preference, and our hope was that the resulting complexes would prove to be reactive at the site *trans* to the amido nitrogen donor. In this regard, BQA-type ligands are conceptually related to the popular family of anionic "pincer" ligands, a class of ligands that now affords a rich reaction chemistry amongst metals from groups 8, 9 and 10.[25] Moreover, it was hoped the aryl organic groups attached to the amide would serve to "soften" otherwise hard ligands and allow for generation of electron-rich organometallic complexes.

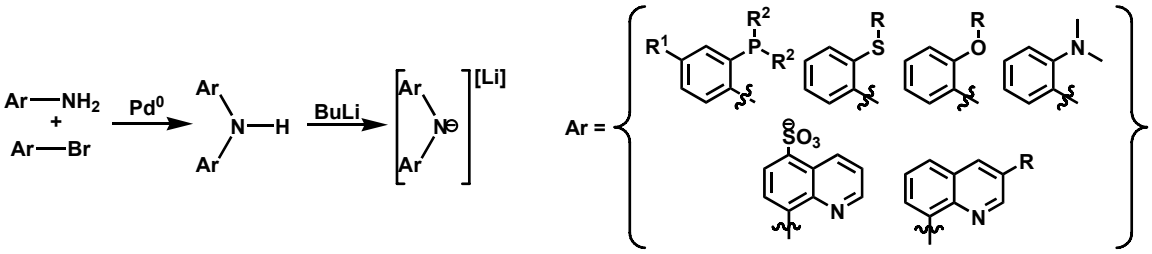

Figure I.5. Generalized ligand synthesis via Pd^0 catalyzed aryl amination.

Deprotonation of (BQA)H with ^{n}BuLi in toluene affords the lithium amide complex $\{(BQA)Li\}_2$, whose dimeric solid-state crystal structure is shown.[22] Crystals of $\{(BQA)Li\}_2$ were obtained and the dimeric structure was established by an X-ray diffraction study (Figure I.6). This Li_2N_2 complex has D_2 molecular symmetry with C_2

axis running through the two lithium atoms in the plane of the parallelepiped formed by N2A, LiB, N2B and LiA (Figure I.6). The dimeric conformation is favored in the absence of a donor solvent and is robust by virtue of each donor arm of the $[BQA]^-$ ligand coordinating to a different lithium center. While the synthesis of $\{(BQA)Li\}_2$ provided us with a useful metathesis reagent for our Group 10 metal studies, it also gave us the first inkling of the potential capacity of this genre of chelating amide to support bridging M_2N_2 diamond core complexes (*vide supra*).

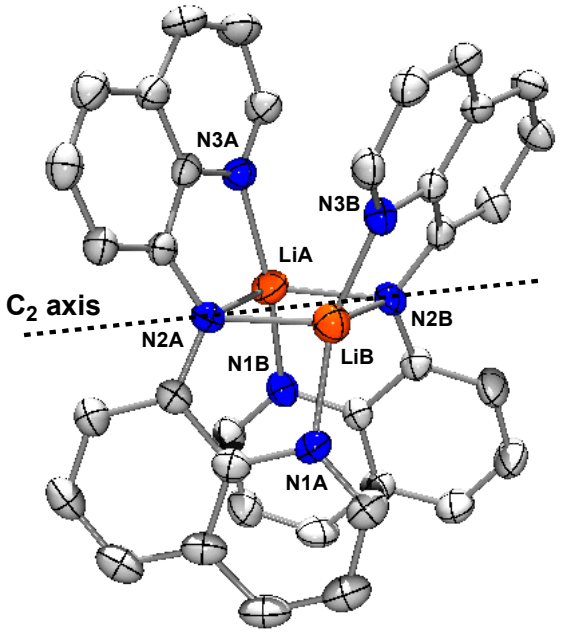

Figure I.6. Displacement ellipsoid (50%) representation of [Li][BQA]. Selected bond distances (Å) and angles (deg) are as follows: LiA-N(1A), 2.024(4); LiA-N(2A), 2.079(4); LiA-N(2B), 2.063(4); LiA-N(3B), 1.990(4); LiA-LiB, 2.395(5); LiB-N(1B), 1.958(4); LiB-N(2B), 2.051(4); LiB-N(2A), 2.018(4); LiB-N(3A), 1.999(4); N(2B)-LiA-N(2A), 107.15(18); N(2A)-LiA-LiB, 53.05(13); N(2B)-LiA-LiB, 54.16(13); N(2B)-LiA-N(2A), 107.15(18); N(1A)-LiA-N(2A), 82.50(15); N(3B)-LiA-N(2A), 103.80(17); C(8A)-N(2A)-C(17A),120.37(17).

Entry into the Group 10 chemistry of (BQA)H was effected by both protolytic and metathetical strategies. The divalent chloride complexes (BQA)PtCl, (BQA)PdCl, and

(BQA)NiCl were prepared and fully characterized.[22] An X-ray structural study for each of these three complexes shows them to be well-defined, square planar complexes in which the auxiliary BQA ligand binds in the expected planar, η^3-fashion. The (BQA)PtMe and (BQA)PtPh complexes were also synthesized and isolated.[26] Both were prepared in excellent yield by transmetallation of $\{(BQA)Li\}_2$ with (COD)PtMeCl and (COD)PtPhCl, respectively, to afford purple microcrystalline solids. Platinum satellites are easily observed in the ^{1}H NMR for both (BQA)PtMe and (BQA)PtPh confirming the attachment of the R group to the Pt center.

Our primary interest in developing these systems was to study the ability of pincer-like amido complexes of platinum to undergo intermolecular C-H bond activation processes. This process is in analogy to the first step of a Shilov-type reaction, in which methane is selectively oxidized to methanol.[27,28] The first step of this mechanism is hypothesized to proceed by a d^8, square planar $[Pt^{II}Cl_4]^{2-}$ reacting with methane, resulting in the formation of a square planar Pt^{II}-CH_3 complex with HCl as the formal by-product; water formally acts as a Bronsted base. By analogy, we sought to examine the activation of benzene by (BQA)PtCl, another robust, d^8, square planar, Pt^{II}-Cl complex. A suspension of (BQA)PtCl in benzene was heated to 150 °C in a sealed reactor, at which time the complex became fully soluble, for several days, and showed no reactivity. A tertiary, sterically encumbering, alkyl amine base, NEt^iPr_2, was then added to examine whether a soluble base would be able to promote reactivity. Again no new Pt products were detected, nor was any of the expected conjugate acid, $[HNEt^iPr_2][Cl]$, evident by ^{1}H NMR.

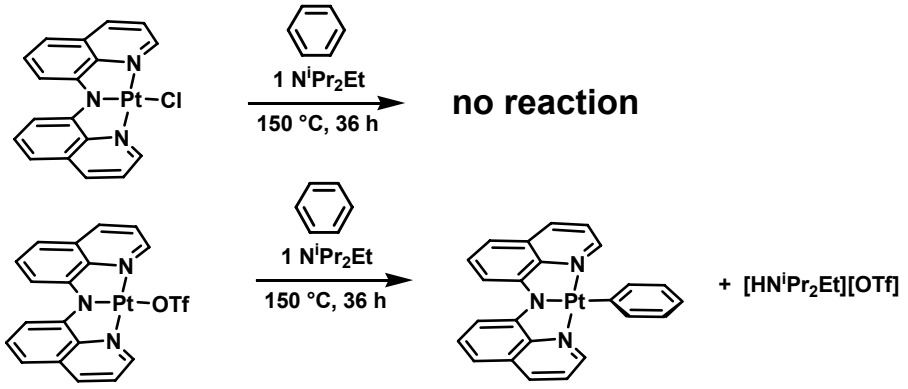

Figure I.7. C-H bond activation by (BQA)Pt^{II}Cl and (BQA)Pt^{II}OTf complexes.

In order to gain entry to a C-H activation system, neutral (BQA)PtOTf was selected because the triflate ligand was anticipated to be much more labile than the corresponding chloride.[26] (BQA)Pt-OTf was also quite insoluble in benzene, however upon heating to 150°C, a red homogeneous solution developed and, after several days, no reactivity was observed. When one equivalent of NEt^{i}Pr$_2$ was added and heating was resumed at 150°C, the expected conjugate acid product [HNEt^{i}Pr$_2$][OTf] became visible by ^{1}H NMR after a few hours (Figure I.7). Further heating for 36 h resulted in consumption of the starting material and a high yield (> 90%) of (BQA)PtPh with a stoichiometric equivalent of [HNEt^{i}Pr$_2$][OTf]. (BQA)PtPh was isolated by column chromatography (70% yield) and identified by ^{1}H-NMR and FAB-MS. At lower temperature (~ 100°C), only 25% conversion to the phenyl product is observed after 5 days, suggesting a very high thermodynamic barrier to the reaction. This barrier is not difficult to reconcile based on the observation of the microscopic reverse in which (BQA)PtOTf is instantly formed upon addition of a stoichiometric amount of triflic acid to (BQA)PtPh at ambient temperature. The (BQA)PtMe complex was also found to undergo oxidation by MeI which afforded the octahedral Pt^{IV} complex (BQA)Pt(Me$_2$)I.

The synthesis and intriguing photoisomerization of the (BQA)Pt^{IV} complex from meridial to facial ligand coordination complexes is described in Appendix A. While many intriguing aspects of Group 10 amide chemistry remain poised for exploration, this path of inquiry was ultimately set aside in order to develop the Group 11 systems described herein.

I.C. References Cited

[1] a) Vallee, B. L.; Williams, R. J. P. *Proc. Natl. Acad. Sci. U.S.A.* **1968**, *59*, 498. b) Rorabacher, D. B. *Chem. Rev.* **2004**, *104*, 651.

[2] Marcus, R. A.; Sutin, N. *Biochim. Biophys. Acta* **1985**, *811*, 265.

[3] (a) Ambundo, E. A.; Yu, Q.; Ochrymowycz, L. A.; Rohrbacher, D. B. *Inorg. Chem*. **2003**, *42*, 5267. (b) Kyritsis, P.; Dennison, C.; Ingeldew, W. J.; McFarlane, W.; Sykes, A. G. *Inorg. Chem*. **1995**, *34*, 5370. (c) Groenveld, C. M.; Canters, G. W. *J. Biol. Chem*. **1988**, *263*, 167. (d) Groenveld, C. M.; Dahlin, S.; Reinhammer, B.; Canters, G. W. *J. Am. Chem. Soc*. **1987**, *109*, 3247.

[4] (a) Solomon, E. I.; LaCroix, L. B.; Randall, D. W. *Pure Appl. Chem*. **1998**, *70*, 799. (b) Randall, D. W.; Gamelin, D. R.; LaCroix, L. B.; Solomon, E. I. *J. Biol. Inorg. Chem*. **2000**, *5*, 16.

[5] (a) Ferguson-Miller, S.; Babcock, G. T. *Chem. Rev*. **1996**, *96*, 2889. (b) Gamelin, D. R.; Randall, D. W.; Hay, M. T.; Houser, R. P.; Mulder, T. C.; Canters, G. W.; de Vries, S.; Tolman, W. B.; Lu, Y.; Solomon, E. I. *J. Am. Chem. Soc*. **1998**, *120*, 5246. (c) George, S. D.; Metz, M.; Szilagyi, R. K.; Wang, H. X.; Cramer, S. P.; Lu, Y.; Tolman, W. B.; Hedman, B.; Hodgson, K. O.; Solomon, E. I. *J. Am. Chem. Soc.* **2001**, *123*, 5757. (d) Ramirez, B. E.; Malmstrom, B. G.; Winkler, J. R.; Gray, H. B. *Proc. Natl. Acad. Sci. U.S.A*. **1995**, *92*, 11949.

[6] (a) Kroneck, P. M. H.; Antholine, W. E.; Riester, J.; Zumft, W. G. *FEBS Lett.* **1989**, *248*, 212. (b) Kroneck, P. M. H.; Antholine, W. E.; Riester, J.; Zumft, W. G. *FEBS Lett.* **1988**, *242*, 70. (c) Antholine, W. E.; Kastrau, D. H. W.; Steffens, G. C. M.; Buse, G.; Sumft, W. G.; Kroneck, P. M. H. *Eur. J. Biochem*. **1992**, *209*, 875.

[7] Williams, P. A.; Blackburn, N. J.; Sanders, D.; Bellamy, H.; Stura, E. A.; Fee, J. A.; McRee, D. E. *Nat. Struct. Biol.* **1999**, *6*, 509.

[8] (a) Houser, R. P.; Young, Jr., V. G.; Tolman, W. B. *J. Am. Chem. Soc.*, **1996**, *118*, 2101. (b) Blackburn, N. J.; deVries, S.; Barr, M. E.; Houser, R. P.; Tolman, W. B.; Sanders, D.; Fee, J. A. *J. Am. Chem. Soc*. **1997**, *119*, 6135. (c) Hagadorn, J. R.; Zahn, T. I.; Que Jr., L.; Tolman, W. B. *J. C. S. Dalton Trans.* **2003**, 1790.

[9] Al-Obaidi, A.; Baranovič, G.; Coyle, J.; Coates, C. G.; McGarvey, J. J.; McKee, V.; Nelson, J. *Inorg. Chem.* **1998**, *37*, 3567.

[10] (a) LeCloux, D. D.; Davydov, R.; Lippard, S. J. *Inorg. Chem*. **1998**, *37*, 6814. (b) LeCloux, D. D.; Davydov, R.; Lippard, S. J. *J. Am. Chem. Soc*. **1998**, *120*, 6810. (c) He, C.; Lippard, S. J. *Inorg. Chem.* **2000**, *39*, 5225.

[11] Gupta, R.; Zhang, Z. H.; Powell, D.; Hendrich, M. P.; Borovik, A. S. *Inorg. Chem.*, **2002**, *41*, 5100.

[12] (a) Nelson J.; McKee, V.; Morgan, G. G. *Prog. Inorg. Chem*. **1998**, *47*, 167. (b) Coyle, J. L.; Elias, H.; Herlinger, E.; Lange, J.; Nelson, J. *J. Biol. Inorg. Chem*. **2001**, *6*, 285.

[13] Dicopper systems structurally distinct from the Cu_2X_2 diamond core motif have in certain cases shown a reversible $Cu^1Cu^1/Cu^{1.5}Cu^{1.5}$ redox process. See, for example, 10c and references therein.

[14] (a) Blackburn, N. J.; Barr, M. E.; Woodruff, W. H.; van der Oost, J.; de Vries, S. *Biochemistry* **1994**, *33*, 10401. (b) Williams, M.; Lapplalainen, P.; Kelly, M.; Sauer-Eriksson, E.; Saraste, M. *Proc. Natl. Acad. Sci. U.S.A*. **1995**, *92*, 11955.

[15] (a) Cui, Ji.; Huang, Q.; Veinot, J. G. C.; Yan, H. Marks, T. J.; *Adv. Mater.* **2002**, *14*, 565. (b) Zhang, Q.; Zhou, Q.; Cheng, Y.; Wang, L.; Ma, D.; Jing, X.; Wang, F. *Adv. Mater.* **2004**, *16*, 432.

[15] Ford, P. C.; Cariati, E.; Bourassa, J. *Chem Rev.* **1999**, *99*, 3625.

[16] McMillin, D. R.; McNett, K. M. *Chem. Rev.* **1998**, *98*, 1201.

[18] Cuttell, D. G.; Kuang, S.-M.; Fanwick, P. E.; McMillin, D. R.; Walton, R. A. *J. Am. Chem. Soc.* **2002**, *124*, 6.

[19] Jenson, K. A.; Nielson, P. H. *Acta Chem. Scand.* **1964**, *18*, 1.

[20] Puzas, J. P.; Nakon, R.; Pertersen, J. L. *Inorg. Chem.* **1986**, *25*, 3837.

[21] (a) Tomori, H.; Sadighi, J. P.; Buchwald, S. L. *J. Org. Chem.* **2000**, *65*, 1158. (b) Wolfe, J. P.; Tomori, H.; Sadighi, J. P.; Yin, J. J.; Buchwald, S. L. *J. Org. Chem.* **2000**, *65*, 1158. (c) Alcazar-Roman, L. M.; Hartwig, J. F.; Rheingold, A. L.; Liable-Sands, L. M.; Guzei, I. A. *J. Am. Chem. Soc.* **2000**, *122*, 4618. (d) Hartwig, J. F. *Accounts Chem. Res.* **1998**, *31*, 852. (e) Hamamm, B. C.; Hartwig, J. F. *J. Am. Chem. Soc.* **1998**, *120*, 12706.

[22] Peters, J. C.; Harkins, S. B.; Brown, S. D.; Day, M. W. *Inorg. Chem.* **2001**, *40*, 5083.

[23] For some relevant lead references see: a) Fryzuk, M. D.; Macneil, P. A.; Rettig, S. J.; Secco, A. S.; Trotter, J. *Organometallics* **1982**, *1*, 918. b) Fryzuk, M. D.; Leznoff, D. B.; Thompson, R. C.; Rettig, S. J. *J. Am. Chem. Soc.* **1998**, *120*, 10126. c) Deacon, G. B.; Gatehouse, B. M.; Grayson, I. L.; Nesbit, M. C. *Polyhedron* **1984**, *3*, 753. d) Buxton, D. P.; Deacon, G. B.; Gatehouse, B. M.; Grayson, I. L.; Wright, P. J. *Acta Crystallogr., Sect. C* **1985**, *41*, 1049. e) Dori, Z.; Eisenberg, R.; Steifel, E. I.; Gray, H. B. *J. Am. Chem. Soc.* **1970**, *92*, 1506. f) Kawamoto, T.; Nagasawa, I.; Kuma, H.; Kushi, Y. *Inorg. Chim. Acta*

1997, *265*, 163. g) Endres, H.; Keller, J.; Poveda, A. *Z. Naturforsch*., *Teil B* **1977**, *32*, 131. h) Sacco, A.; Vasapollo, G.; Nobile, C. F.; Piergiovanni, A.; Pellinghelli, M. A.; Lanfranchi, M. *J. Organomet. Chem.* **1988**, *356*, 397.

[24] a) Vila, J. M.; Pereira, M. T.; Ortigueira, J. M.; Lata, D.; Torres, M. L.; Fernandez, J. J.; Fernandez, A.; Adams, H. *J. Organomet. Chem*. **1998**, *566*, 93. b) Crespo, M.; Solans, X.; Font-Bardia, M. *Polyhedron* **1998**, *17*, 3927. c) Gandelman, M.; Vigalok, A.; Shimon, L. J. W.; Milstein, D. *Organometallics* **1997**, *16*, 3981.

[25] a) Liu, F. C.; Pak, E. B.; Singh, B.; Jensen, C. M.; Goldman, A. S. *J. Am. Chem. Soc.* **1999**, *121*, 4086. b) Sundermann, A.; Uzan, O.; Milstein, D.; Martin, J. M. L. *J. Am. Chem. Soc.* **2000**, *122*, 7095. c) Dani, P.; Karlen, T.; Gossage, R. A.; Gladiali, S.; van Koten, C. *Angew. Chem. Int. Ed.* **2000**, *39*, 743.

[26] Harkins, S. B.; Peters, J. C. *Organometallics* **2002**, *21*, 1753.

[27] Shilov, A. E.; Shul'pin, G. B. *Chem. Rev.* **1997**, *97*, 2879.

[28] a) Stahl, S. S.; Labinger, J. A.; Bercaw, J. E. *J. Am. Chem. Soc.* **1996**, *118*, 5961. b) Stahl, S.; Labinger, J. A.; Bercaw, J. E. *Angew. Chem. Int. Ed.* **1998**, *37*, 2181.

Chapter II

Electrochemical Studies of Dicopper Complexes Supported by Bis(2-tertbutylsulfanylphenyl)amido Ligands [†]

[†]Adapted from Harkins, S. B.; Peters, J. C. *J. Am. Chem. Soc.* **2004**, *126*, 2885.

II.A. Introduction

Biological electron transfer agents that feature copper are most typically mononuclear in nature, as observed in the well known "blue copper" family of proteins.[1,2,3] Such systems and relevant small molecule model complexes have been studied intensively to gain an appreciation of how the inner coordination geometry of a copper ion dictates its ability to mediate rapid electron transfer.[4] While the issues that dictate electron transfer rates in copper proteins are an ongoing topic of concern,[4a,5] it is widely accepted that structural reorganization needs to be minimized to achieve rapid rates.[6]

Higher nuclearity copper-based electron transfer agents, while less common, are now well established. For example, a collection of spectroscopic and more recent structural data has revealed that cytochrome *c* oxidase accomplishes enhanced electron transfer (ET) into and out of a buried Cu_A site by virtue of a highly covalent, thiolate-bridged Cu_2S_2 diamond core structure type.[7,8] Amongst the various low molecular weight systems that have been developed to model aspects of this Cu_A site,[9,10,11,12] perhaps the most structurally relevant concerns Tolman's thiolate-bridged, mixed-valence $\{L^{N3S}Cu^{1.5}\}_2^+$ diamond core complex.[9a] This complex features an EPR signal consistent with a fully delocalized class III diamond core description,[7b,9a] as observed for the resting state form of Cu_A.[7b,8] Despite this similarity, the Cu···Cu distance in the Tolman model system is much larger than that observed in Cu_A, and the complex does not reproduce the reversible Cu^1Cu^1 to $Cu^{1.5}Cu^{1.5}$ redox behavior of Cu_A. Several dicopper systems that diverge from the diamond core structural motif do show reversible redox behavior for a $Cu^{1.5}Cu^{1.5}$ mixed-valence state.[11c,13] For example, a family of dicopper azacryptates has been developed that successfully brings two copper centers constrained by the

azacryptate cage into much closer proximity (~ 2.35 – 2.4 Å).[13a] Some of these complexes, which are characterized by a direct metal-metal σ bond that is quite distinct from the bonding situation in Cu_A, nonetheless exhibit very rapid electron self-exchange (k_s) between their oxidized and reduced forms (~ 10^5 M^{-1} s^{-1}).[13b]

Yet to be developed are *diamond core* copper systems that can reversibly model *both* the reduced Cu^ICu^I and the delocalized $Cu^{1.5}Cu^{1.5}$ redox states observed in Cu_A.[14] Ligand systems that would help to minimize structural reorganization between these two redox forms, and hold the two copper centers of a diamond core in close enough proximity to reproduce the short Cu-Cu bond distance observed in Cu_A (~ 2.5 Å),[15] might serve as simplified functional models for the redox behavior of Cu_A.[7b,c,d] One avenue into this regime using small molecule design is to replace the thiolate bridging units inherent to the Cu_2S_2 diamond core of Cu_A with amido bridging units. Such a strategy should slide the copper centers closer together so as to better model the distance observed in Cu_A while still maintaining a Cu_2X_2 diamond core motif. Moreover, such an approach might shed some light on whether thiolate plays a unique role in facilitating rapid electron transfer chemistry by bringing two copper centers of a diamond core into strong electronic communication. Herein we describe a Cu_2N_2 diamond core system supported by sulfur-rich, tridentate amido ligands that exhibits a fully reversible and very facile 1-electron redox process between a Cu^1Cu^1 and a class III delocalized $Cu^{1.5}Cu^{1.5}$ form. Solid-state structural snapshots of both redox forms are described that reveal (i) very short Cu···Cu distances akin to those in Cu_A, and (ii) minimal structural reorganization upon oxidation from the reduced Cu^1Cu^1 to the delocalized $Cu^{1.5}Cu^{1.5}$ state. These features facilitate very facile rates of electron self-exchange between the reduced and one

electron oxidized forms of the system ($\geq 10^7$ M^{-1} s^{-1}), rates which to our knowledge are faster than those measured for other low molecular weight copper complexes.[4a,13b] A distinct Cu···Cu compression accompanies the 1-electron oxidation process that may reflect the onset of direct Cu-Cu electronic exchange.

II.B. Results and Discussion

Scheme II.1

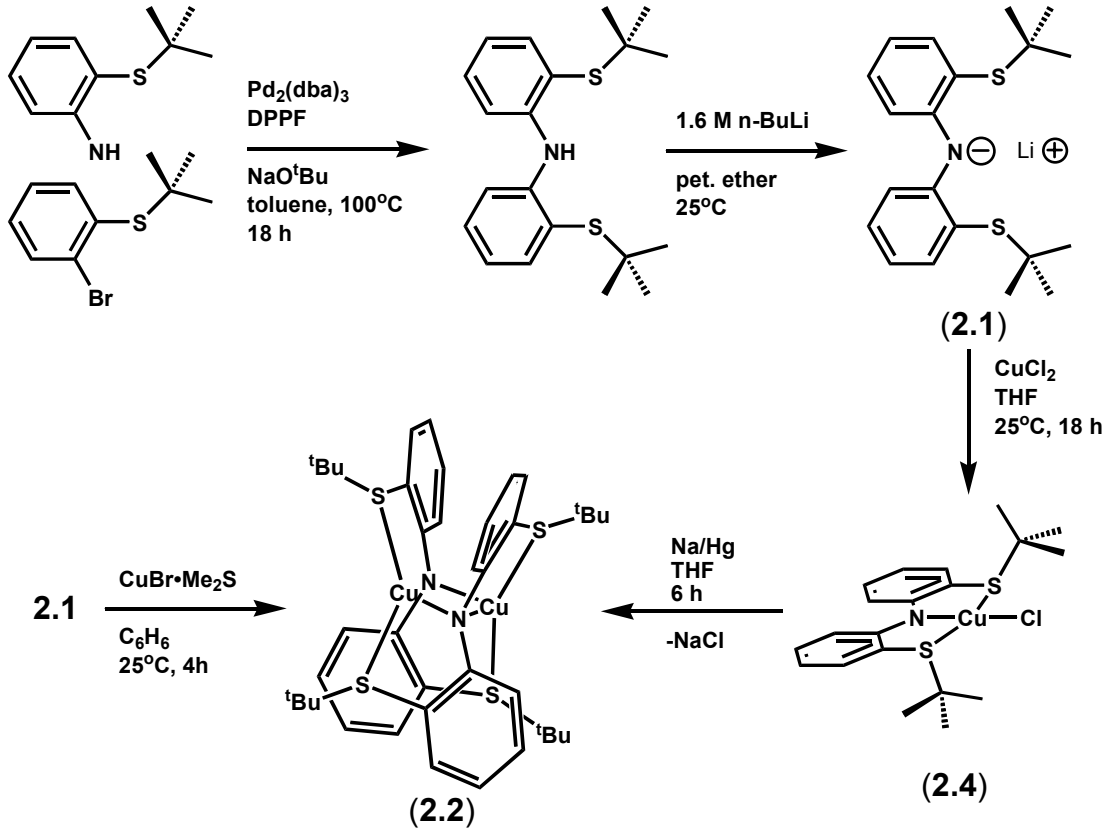

Palladium(0) cross-coupling of 2-*tert*-butylsulfanyl bromobenzene with 2-*tert*-butylsulfanyl aniline afforded bis(2-*tert*-butylsulfanylphenyl)amine in 87% isolated yield.[16,17] Addition of ^{n}BuLi to the purified amine provided its lithium salt, abbreviated as [SNS][Li] (**2.1**) (Scheme II.1). Access to a diamagnetic dicopper(1,1) complex was accomplished by reaction of **2.1** with CuBr·Me_2S in benzene. Analytically pure yellow

needles were obtained by recrystallization of the crude product from dichloromethane, and XRD analysis established the dimeric species $\{[SNS][Cu]\}_2$ (**2.2**) shown in Figure II.1. Addition of a stoichiometric amount of $[Cp_2Fe][B(3,5\text{-}(CF_3)_2C_6H_3)_4]$ to **2.2** produced the dinuclear complex $[\{[SNS][Cu]\}_2][B(3,5\text{-}(CF_3)_2C_6H_3)_4]$ (**2.3**), which exhibits a temperature-independent magnetic moment between 10 and 295 K (μ_{eff} = 1.54 μ_B at 75 K (SQUID)). Analytically pure **2.3** was isolated as red-brown crystals by crystallization from a petroleum ether/diethyl ether mixture. Employing a Cu(II) source provided access to a mononuclear copper(II) complex supported by the [SNS] ligand scaffold. This was accomplished by stirring a slurry of **2.1** and $CuCl_2$ in THF for 18 h, after which time the square-planar copper complex [SNS]CuCl (**2.4**) was isolated as a deep green solid. X-ray quality crystals were obtained by recrystallization from THF/petroleum ether at –30 ºC and the solid-state structure of **2.4** is shown in Figure II.2. Of note from the structure are the orientation of the *tert*-butyl groups, which are directed towards opposite faces of the square plane, and the canted nature of the aryl rings. These features provide the complex with molecular C_2 symmetry. The Cu-N bond distance is 1.915(2) Å, and the Cu-S1 and Cu-S2 bond distances are 2.3476(7) Å and 2.3465(7) Å, respectively. Few amido complexes of copper(II) have been prepared for comparison of the Cu-N bond distance. Perhaps the most relevant complex is [BQA]CuCl (BQA = bis(8-quinolinyl)amido),[18] which features a Cu-N(amido) distance of 1.935(2) Å. The Cu-S distances in **2.4** appear to be typical for Cu(II) based upon an analysis of data stored in the Cambridge Structural Database (CSD, avg. = 2.38 Å).[19] The EPR spectrum of **2.4**, which is shown in Figure II.3, confirms its expected S = 1/2 spin state. The reduction of **2.4** by 1.05 equivalents of Na/Hg amalgam in THF provides an alternative synthesis of the dicopper complex **2.2**.

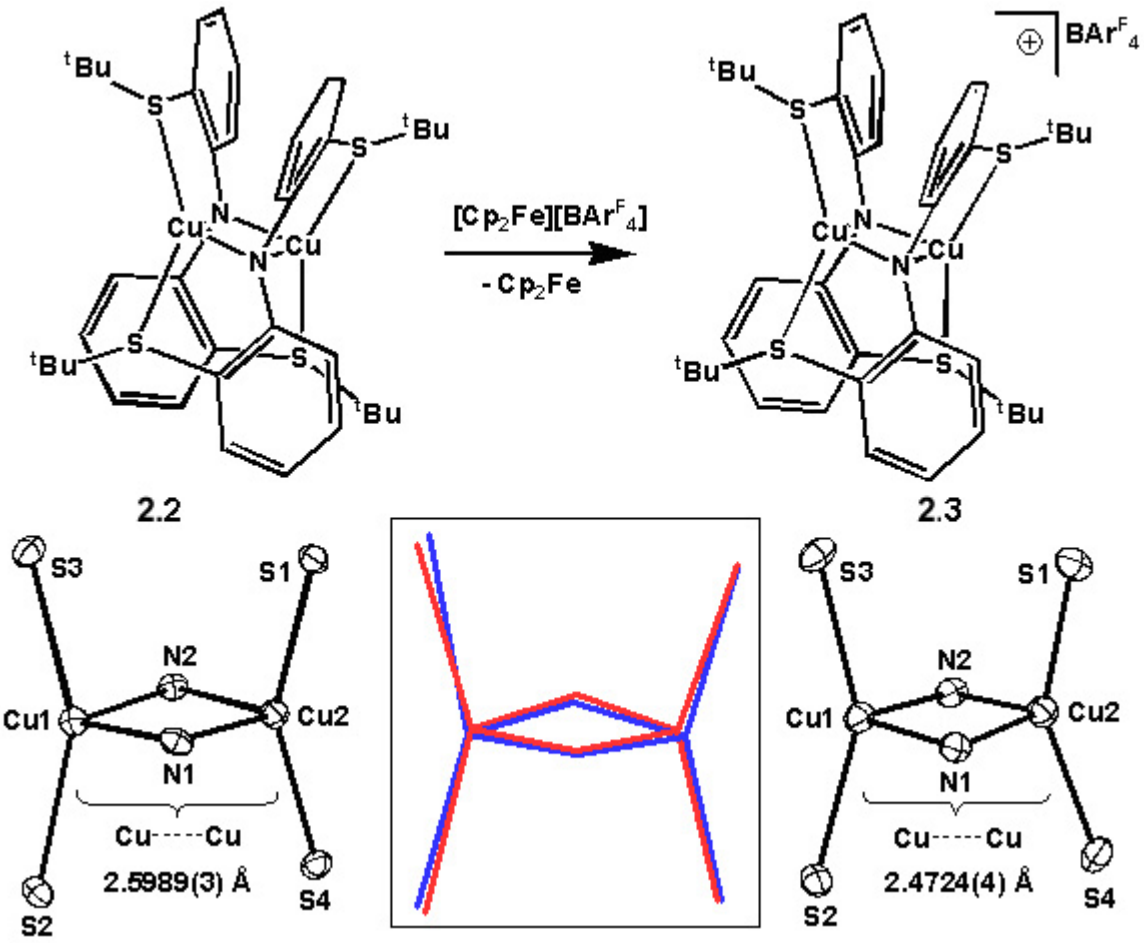

Figure II.1. Molecular representations (top) of **2.2** and **2.3** (BAr^F_4 = $B(3,5\text{-}(CF_3)_2C_6H_3))_4$. Displacement ellipsoid representations (50%) of the core atoms of **2.2** (*bottom left*) and **2.3** (*bottom right*), and graphical overlay (center; **2.2** in red; **2.3** in blue). Selected bond lengths (Å) and angles (º): For **2.2** vs. **2.3**: Cu1-Cu2, 2.5989(3) vs. 2.4724(4); Cu1-N1, 2.1149(14) vs. 2.0887(16); Cu1-N2, 2.1303(14) vs. 2.1011(17); Cu2-N1, 2.0850(14) vs. 2.0641(16); Cu2-N2, 2.1395(14) vs. 2.0568(16); Cu1-S2, 2.2730(5) vs. 2.2805(6); Cu1-S3, 2.2854(5) vs. 2.2805(6); Cu2-S4, 2.2735(5) vs. 2.2797(6); Cu2-S1, 2.2853(5) vs. 2.2834(6); Cu2-N1-Cu1, 76.45(5) vs. 73.07(5); Cu1-N2-Cu2, 74.99(5) vs. 72.96(5); S2-Cu1-S3, 152.921(19) vs. 150.50(2); S4-Cu2-S1, 153.233(19) vs. 150.71(2); N1-Cu1-N2, 103.88(5) vs. 105.53(6); N2-Cu2-N1, 104.59(5) vs. 108.04(5).

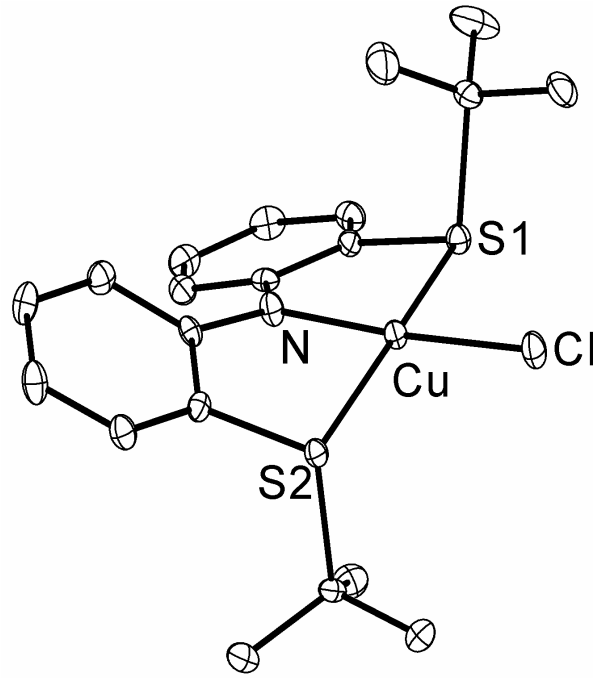

Figure II.2: Solid state molecular structure of **2.4** (50% displacement ellipsoids). The protons have been removed for clarity. Selected bond lengths (Å) and angles (º): Cu-N, 1.915(2); Cu-Cl, 2.2068(7); Cu-S1, 2.3476(7); Cu-S2, 2.3465(7); N-Cu-Cl, 173.44(7); S1-Cu-S2, 167.35(3); N-Cu-S1, 86.02(6); N-Cu-S2, 86.37(6); S1-Cu-Cl, 95.89(2); S2-Cu-Cl, 92.80(2).

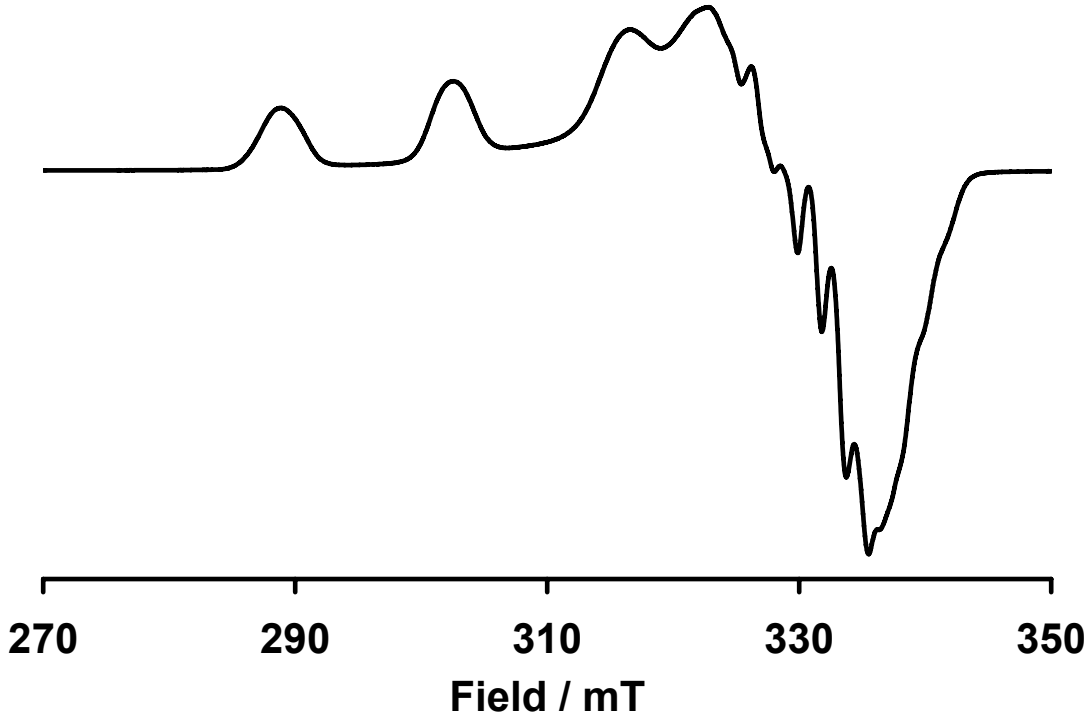

Figure II.3: X-band EPR spectrum (9.40 GHz) of **2.4** at 77 K in 2-methyltetrahydrofuran.

The solid-state structures of complexes **2.2** and **2.3** are unique and of central interest in this paper. A common, dinuclear Cu_2N_2 diamond core structure type featuring anionic amido (NR_2^-) bridging units is observed for each complex (Figure II.1). The four-coordinate copper centers of both **2.2** and **2.3** are quite distorted from idealized tetrahedra and are perhaps better described as cis-divacant octahedra. In this latter formulation, the thioether donors occupy the two axial sites (avg. S-Cu-S angle: 153º for **2.2**; 150.5º for **2.3**) and the amido bridges the two equatorial sites (avg. Cu-N-Cu angle: 75.8º for **2.2**; 73.0º for **2.3**). The two sulfur donors common to each amido bridge bind such that each coordinates a different copper center, thereby providing idealized D_2 symmetry to each system. The distinct ligand binding motifs between structures **2.2** and **2.3** and the square planar complex **2.4** underscore the coordinative flexibility of the $[SNS]^-$ ligand.

The high structural similarity between the reduced and oxidized forms of **2.2** and **2.3**, clearly evident from the graphical overlay of their cores that is shown in Figure II.1, is to our knowledge unprecedented in a dicopper diamond core model system. Close inspection of the bond distances of the core atoms of **2.2** and **2.3** does expose several noteworthy differences. Foremost amongst these is the marked shortening of the Cu···Cu distance in **2.3** (2.472 Å) by comparison to that of **2.2** (2.599 Å), a net change of ~ 0.13 Å. The short Cu···Cu distance observed for **2.3** is nearly identical to that observed for the mixed-valence form of Cu_A in cytochrome *c* oxidase. The Cu-N bond distances in **2.3** are on average slightly shorter than in **2.2** (avg. for **2.3** = 2.08 Å; avg. for **2.2** = 2.12 Å), and the Cu-N-Cu angles become slightly more acute (by approximately 2º) as the copper centers slide closer together. Interestingly, despite the contraction of the Cu_2N_2

core, the Cu-S bond distances remain effectively unchanged (the average of the Cu-S distances for both **2.2** and **2.3** is 2.28 Å).

Complex **2.2** exhibits a fully reversible redox process at –390 mV in CH_2Cl_2 (Fc^+/Fc, 0.30 M [$^nBu_4N$][PF_6], 50 mV/s) that we assign as the $Cu^{1.5}Cu^{1.5}/Cu^1Cu^1$ redox couple (Figure II.4).[20] The redox process is also reversible in THF solution at -250 mV (Fc^+/Fc, 0.35 M [$^nBu_4N$][PF_6], 50 mV/s). An irreversible redox process[21] is observed at much higher potential in CH_2Cl_2 (E_{pa} = +560 mV) and in THF (E_{pa} ~ +570 mV) that most likely reflects oxidation to an unstable dicopper(II,II) species. The large difference in the anodic potentials (880 mV in CH_2Cl_2) between these waves suggests the possibility of strong stabilization of the $C^{1.5}Cu^{1.5}$ form due to class III delocalization. EPR data presented below supports this assertion.

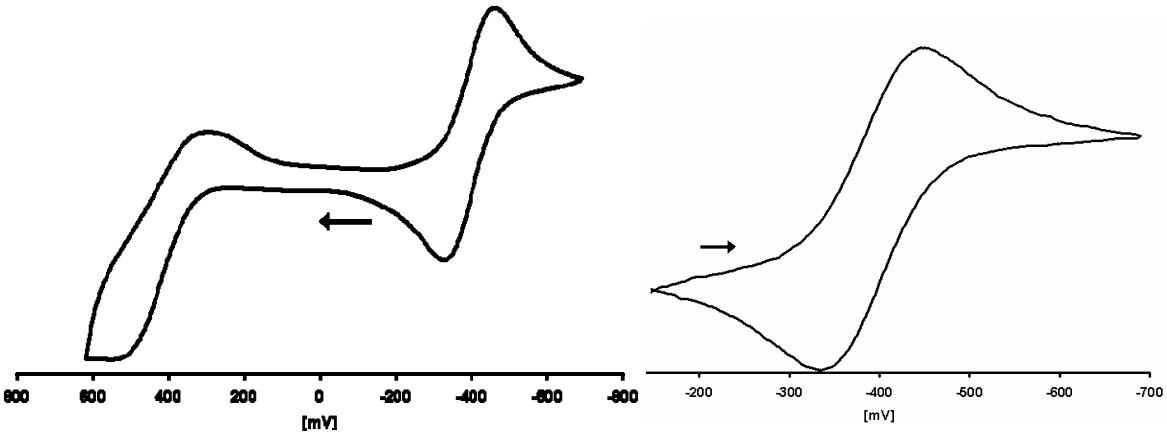

Figure II.4: Cyclic voltammetry of **2.2** referenced vs. Fc^+/Fc in CH_2Cl_2 (0.10 M [$^nBu_4N$][PF_6]. *Left*, **2.2** (80 mV/s); *right,* **2.2** in CH_2Cl_2 (50 mV/s).

The optical spectrum of yellow **2.2** (Figure II.5) was recorded in the range between 24 000 and 4000 cm^{-1} and shows a single, fairly intense absorption at 23 000 cm^{-1} (ε = 3900 $M^{-1}cm^{-1}$). The optical spectrum of **2.3** (Figure II.5) in this range is much richer. While its spectrum is clearly unique from that obtained for Cu_A and related mixed-valence model complexes, it does contain several gross features that may be related to

some of the absorption features recorded for these other systems.[7b] For example, a low energy near-IR absorption at 8550 cm^{-1} ($\varepsilon = 2050\ M^{-1}cm^{-1}$ in CD_2Cl_2) is observed for **2.3** that lies slightly to the blue of a band that has been assigned as the $\Psi \rightarrow \Psi^*$ transition of $\{L^{N3S}Cu^{1.5}\}_2^+$ (6760 cm^{-1} in solution).[7b] At slightly lower energy, an appreciably more intense absorption is observed (5240 cm^{-1}; $\varepsilon = 4700\ M^{-1}cm^{-1}$ in CD_2Cl_2) in the spectrum for **2.3** which appears to be unique from those spectra obtained for Cu_A and relevant model complexes. Another intriguing band of fairly low intensity is centered around 13400 cm^{-1} (ε_{max} = 600 $M^{-1}cm^{-1}$). This feature appears to be a superposition of two uniquely defined absorptions. Several broad features are also evident at higher energy between 16000 and 24000 cm^{-1}. The optical spectrum of square planar **2.4** shows two broad and relatively weak transitions, one centered at 15000 cm^{-1} (ε = 320 $M^{-1}cm^{-1}$) and one at 7800 cm^{-1} ($\varepsilon = 280\ M^{-1}cm^{-1}$).

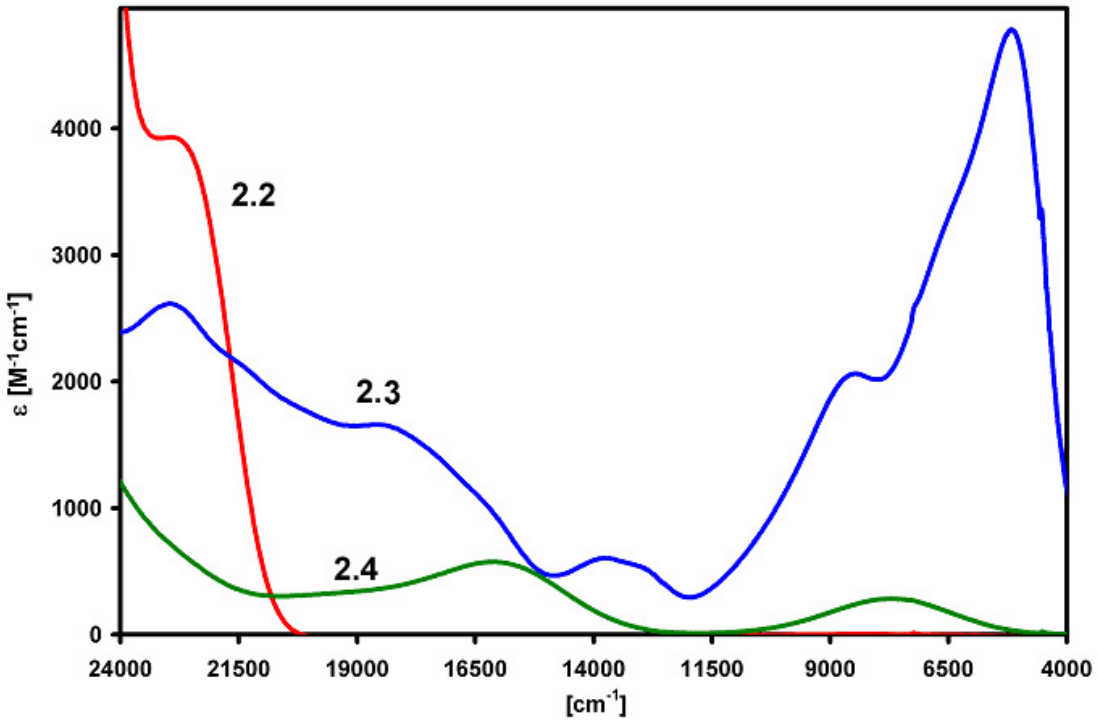

Figure II.5: Electronic absorption spectrum of **2.2** (red), **2.3** (blue), and **2.4** (green) in methylene chloride-d_2.

For comparison, the lowest energy band of Cu_A, which has been assigned as the $\Psi \rightarrow \Psi^*$ transition, is observed at 13,400 cm^{-1}.[7b] The significant energy difference in the $\Psi \rightarrow \Psi^*$ transition between $\{L^{N3S}Cu^{1.5}\}_2^+$ and Cu_A has been attributed to the significant difference in their respective Cu-Cu distances. The distance in $\{L^{N3S}Cu^{1.5}\}_2^+$ is 2.92 Å, and that in Cu_A is ~ 2.5 Å.[7b] Whereas direct Cu-Cu π overlap is possible for Cu_A, no direct exchange is presumably operative in $\{L^{N3S}Cu^{1.5}\}_2^+$ owing to its much larger internuclear distance. Given these data, it would certainly be of interest to determine the origin of the bands centered at ~ 13,400 cm^{-1} for **2.3**, or those lower energy features centered around 8600 cm^{-1} and 5240 cm^{-1}. In particular, it is of interest to determine which of these, if any, arises from a $\Psi \rightarrow \Psi^*$ transition given that this latter complex features a Cu-Cu distance that is very similar (2.4724(4) Å) to that observed in Cu_A.

A geometry optimization and electronic structure calculation of **2.3** using DFT (JAGUAR 5.0, B3LYP/LACVP**) was performed using the crystallographically determined X-ray coordinates as the initial geometry guess.[22] The calculation provided a theoretically determined structure whose geometry agreed remarkably well with the experimental structure. The electronic structure of **2.3** afforded by the DFT calculation suggests that the redox active SOMO (Figure II.6) contains significant orbital contributions from the four atoms of the Cu_2N_2 diamond core. The SOMO is antibonding with respect to each of the four Cu-N interactions and also the Cu-Cu interaction. This phase pattern is consistent with the observed Cu_2N_2 core expansion that occurs when this orbital becomes doubly occupied by reduction to the Cu^1Cu^1 species **2.2**. The SOMO shown in Figure II.6 shows a phase relationship similar to that calculated for the SOMO

Figure 2.6: DFT minimized structure of 2.3 and contour plot (value = 0.065) of the singly occupied molecular orbital (SOMO) and fourteen highest energy filled orbitals.

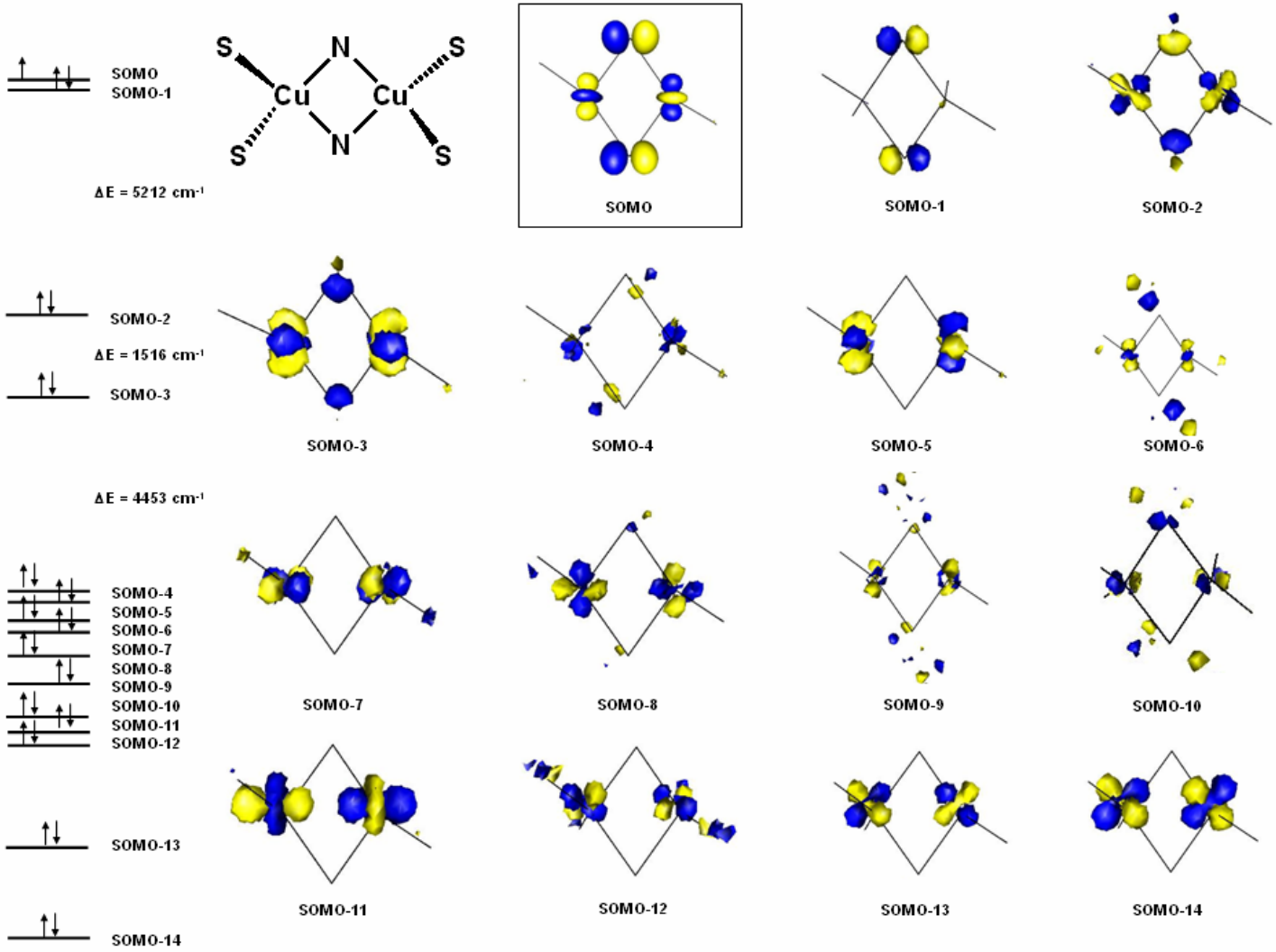

of a thiolate-bridged dicopper site of Cu_A.[7c] The next fourteen highest energy occupied orbitals are also shown to enhance the orbital description.

The X-band EPR spectrum of **2.3** was obtained in 2-methyltetrahydrofuran in the temperature range between 5 K and 80 K (Figure II.7). The data obtained are fully consistent with describing the system as a class III mixed-valence species. The EPR signal observed, which retains its structure from 5 K to 80 K, displays 7-line hyperfine coupling due to the dicopper core, as expected for a system featuring one unpaired electron that is coupled to two copper centers. While super-hyperfine coupling to the bridging nitrogen nuclei of the Cu_2N_2 core might be anticipated, such coupling is not readily discerned in the X-band spectra. We attempted to simulate the experimental EPR spectrum for **2.3** acquired at 5.2 K and simulated the spectrum. The difficulty with simulating the spectrum does not appear to be due to a trace copper(II) impurity: the spectrum shown proved highly reproducible using samples that had been independently synthesized and recrystallized. Moreover, the EPR spectrum of complex **2.4** shown in Figure II.3 is typical of copper(II) complexes supported by the $[SNS]^-$ ligand, and similar features are not present in the spectrum of **2.3**. The three g tensors in the spectrum of **2.3** are poorly resolved (g_x = 1.998, g_y = 2.065, g_z = 2.067, A_x^{Cu} = 3 G, A_y^{Cu} = 18.4 G, A_z^{Cu} = 44.5 G), and this makes the simulation difficult. Acquisition of the EPR spectrum of **2.3** at higher field strength should help to resolve the spectrum. The experimental EPR data and our crude simulation do nonetheless support assignment of **2.3** as an S = ½ system coupled to a symmetric dicopper center.

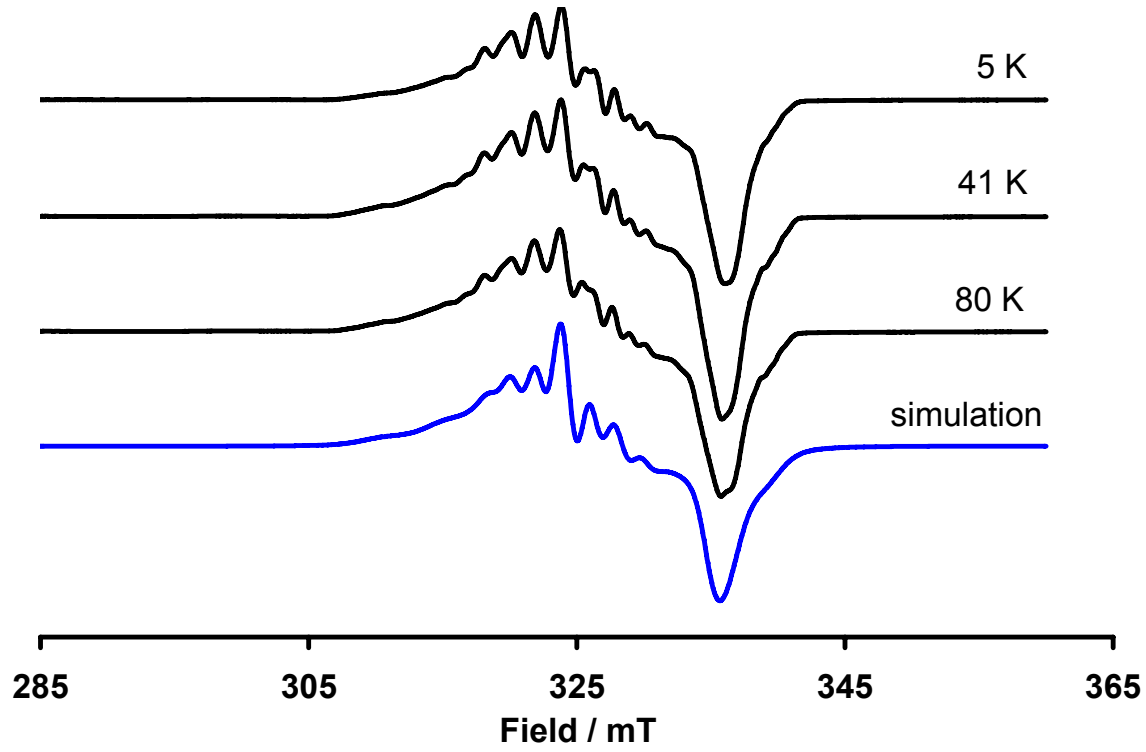

Figure II.7: X-band EPR spectrum (9.38 GHz) of **2.3** at 80 K , 41 K, and 5 K in 2-methyltetrahydrofuran (black). Simulated spectrum (blue) {g_x = 1.998, g_y = 2.065, g_z = 2.067, A_x^{Cu} = 3 G, A_y^{Cu} = 18.4 G, A_z^{Cu} = 44.5 G}.

Given the small structural reorganization that occurs upon oxidation of **2.2** to **2.3**, and the reversibility of the process, we reasoned that unusually rapid intermolecular electron transfer kinetics might be observable in the present system. Whereas electron transfer kinetics at biological copper sites and low molecular weight copper complexes have been the subject of many previous studies,[4,13,23] in part motivated by the rapid electron transfer rates obtained in type 1 copper sites of blue copper proteins,[4b,c,d] to our knowledge such studies have not included diamond core dicopper model systems. We therefore sought to measure, or at least approximate, the intermolecular self-exchange rate between **2.2** and **2.3** directly using the technique of ^{1}H NMR line-broadening analysis.[24]

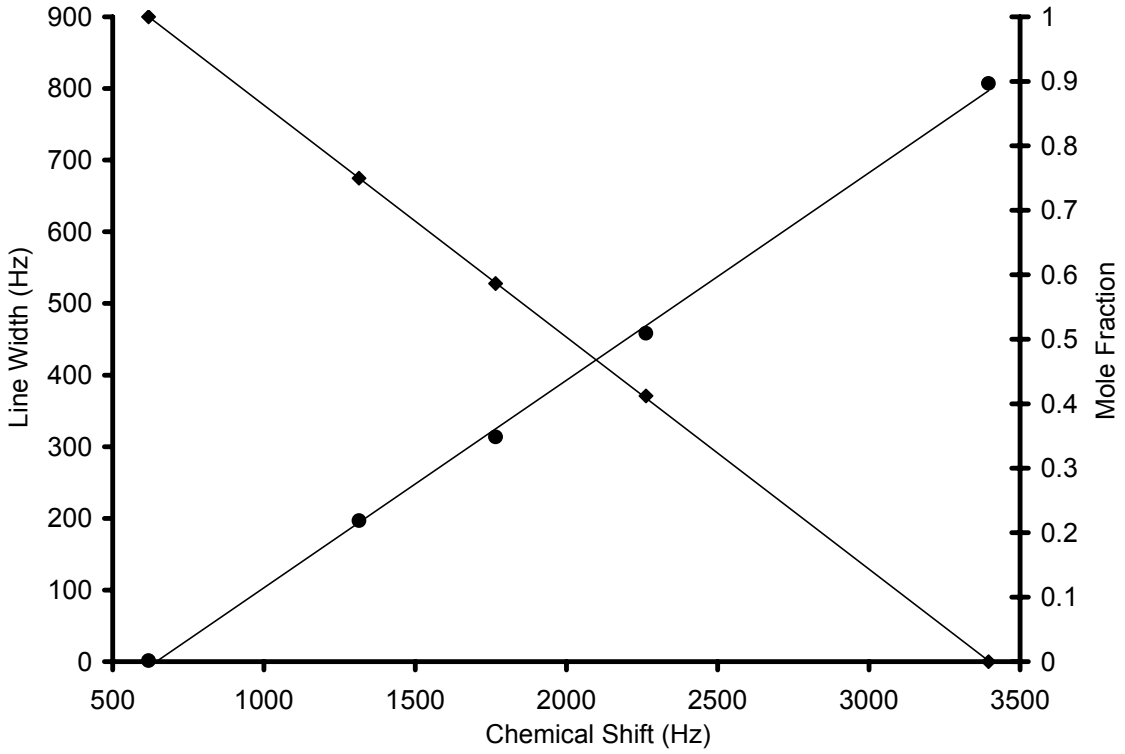

Graph II.1: Plots of line width vs. chemical shift (◆) and mole fraction vs. chemical shift (●).

A single and sharp resonance for the *tert*-butyl protons of **2.2** is observed at 1.23 ppm. For a pure sample of **2.2** its line width W_2 (where line width indicates the full-width at half maximum for the Lorentzian-shaped line) is 1.3 ± 0.2 Hz. The ^{1}H NMR spectrum of a pure sample of **2.3** features a very broad resonance centered at 6.79 ppm. This resonance is slightly convoluted by overlap with the aryl protons of the [B(3,5-$(CF_3)_2C_6H_3)_4$] counter-anion. Nonetheless its line width, W_3, can be estimated as 807 ± 25 Hz. The addition of increasing amounts of cationic **2.3** to a solution of **2.2** in CD_2Cl_2 causes the observed resonance to broaden and to shift downfield. A plot of the chemical shift of this resonance as a function of the mole fraction of **2.2**, χ_2, reveals a linear correlation (Graph II.1) and therefore suggests that the rate of electron-exchange between **2.2** and **2.3** falls within the fast-exchange regime. If we assume a two-site exchange

system comprised of diamagnetic **2.2** and paramagnetic **2.3**, and if the rate law for electron-transfer is first order with respect to each reactant concentration, then equation II.1 relating line widths and reactant lifetimes holds:[25,26]

$$W_{23} = \chi_3 W_3 + \chi_2 W_2 + [\chi_3\chi_2\{4\pi(\delta\nu)^2 k_s^{-1} C_{23}^{-1}\}] \quad \text{(II.1)}$$

In this equation $\delta\nu$ represents the contact shift between **2.2** and **2.3**, k_s represents the rate constant for electron self-exchange (M^{-1} s^{-1}), and C_{23} represents the total molarity of the solution of **2.2** and **2.3**. To obtain a reliable value for k_s in the fast exchange region, it is necessary that W_{23} be considerably larger than the sum $\{\chi_3 W_3 + \chi_2 W_2\}$. When k_s approaches very high values ($>10^8$ M^{-1} s^{-1}), the third term $[\chi_3\chi_2\{4\pi(\delta\nu)^2 k_s^{-1} C_{23}^{-1}\}]$ approaches zero and W_{23} converges to the sum $\{\chi_3 W_3 + \chi_2 W_2\}$. Within the error estimated for our line width measurements W_2, W_3, and W_{23}, the magnitude of W_{23} is too close to the sum $\{\chi_3 W_3 + \chi_2 W_2\}$ to accurately determine the magnitude of k_s. In other words, small errors in our values for W_2, W_3, and W_{23} will dramatically affect the value predicted. Therefore the rate of the exchange process is too fast to measure accurately by the technique of NMR line-broadening analysis, and we must at present be satisfied with suggesting a conservative lower boundary limit for k_s as $\geq 10^7$ M^{-1} s^{-1}. We attempted to slow the exchange rate down by diluting the total concentration of **2.2** and **2.3**, but the line widths W_{23} obtained were still too close to the sum $\{\chi_3 W_3 + \chi_2 W_2\}$ to provide accurate values for k_s. The crude lower boundary we estimate for k_s can be compared to that measured for Fc/[Fc][PF_6] (Fc = ferrocene) by the same technique (k_s = (4.3 ± 0.3) x 10^6 M^{-1} s^{-1} at 298 K in CD_2Cl_2).[24c] More interesting is to consider values that have been measured for Cu_A for comparison. While electron self-exchange rates are obviously not available for the buried Cu_A site of cytochrome *c* oxidase, meaningful values for electron

transfer rates into and out of Cu_A domains have been measured. Perhaps the most meaningful value for comparison to the present model system is that determined by Slutter et al. using flash photolysis to initiate electron transfer between excited (2,2'-bipyridyl)ruthenium(II) ($Ru^{II}(bpy)_3$*) and the soluble Cu_A domain from the cytochrome ba_3 of *Thermus thermophilus*.[27] The value estimated in that study for the second-order ET rate constant from $Ru^{II}(bpy)_3$* to the fully oxidized Cu_A site at high ionic strength was determined to be 2.2 x 10^8 M^{-1} s^{-1}. Stopped flow studies with a soluble Cu_A domain and its natural partner cytochrome c_{550} from *P. denitrificans* provided rates of 1.5 x 10^6 M^{-1} s^{-1}.[28] Electron self-exchange values determined for the oxidized and reduced forms of plastocyanin from *Anabaena variabilis* obtained by longitudinal NMR relaxation were 1.50 ± 0.13 x 10^5 M^{-1} s^{-1} at 298 K in pH 7.0 H_2O.[29] Clearly, the lower boundary for k_s we have proposed suggests our model system can achieve electron-transfer rates comparable to Cu_A. It is therefore of obvious interest to more accurately determine an ET value for the present Cu_2N_2 model system for direct comparison to a known value for a soluble Cu_A domain. Efforts are now underway to examine the flash photolysis methodology used by Slutter et. al. to determine whether this will be a viable strategy.

To conclude, the amido-bridged Cu_2N_2 diamond core structures described herein provide an interesting structural departure from the thiolate-bridged diamond cores of biological Cu_A. Nonetheless, the $\{[SNS][Cu]\}_2^{+n}$ (n = 0, 1) system is unique amongst *dicopper diamond cores* in its ability to functionally model both the reduced and the one-electron oxidized mixed-valence states of biological Cu_A. Minimal structural reorganization of the $[SNS]^-$ ligand framework, and the short Cu-Cu distance it supports, are likely important factors governing the reversible redox behavior of $\{[SNS][Cu]\}_2^{+n}$.

Moreover, these same factors seem to provide access to a very facile $Cu^{1}Cu^{1} \leftrightarrow Cu^{1.5}Cu^{1.5}$ electron self-exchange process ($\geq 10^{7}$ M^{-1} s^{-1}), the lower limit of whose magnitude is to our knowledge unprecedented in copper model complexes. These data collectively suggest that amido bridges are an attractive alternative to thiolate as a bridging unit for dicopper diamond core systems, especially if a facile electron transfer agent is desired. Many questions remain to be answered for the dicopper systems discussed herein, and future studies will probe the spectroscopy and electron-transfer kinetics of these new systems in more detail. Moreover, we will explore whether synthetic access to related Cu_2N_2 structure types using other $[LNL]^{-}$ ligands is possible so as to probe structure/function relationships in such systems more thoroughly.

II.C. Experimental

General. All manipulations were carried out using standard Schlenk or glove-box techniques under a dinitrogen atmosphere. Unless otherwise noted, solvents were deoxygenated and dried by thorough sparging with N_2 gas followed by passage through an activated alumina column. Non-halogenated solvents were tested with a standard purple solution of sodium benzophenone ketyl in tetrahydrofuran to confirm effective oxygen and moisture removal. All reagents were purchased from commercial vendors and used without further purification unless otherwise stated. 2-*tert*-butylsulfanyl aniline,[30] $[Cp_2Fe][B(3,5\text{-}(CF_3)_2C_6H_3)_4]$,[31] and $CuCl_2 \cdot 0.66$ THF[32] were prepared according to literature procedures. Elemental analyses were performed by Desert Analytics, Tucson, AZ. Deuterated solvents were purchased from Cambridge Isotope Laboratories, Inc. and degassed and dried over activated 3 Å molecular sieves prior to use. A Varian Mercury-300 or INOVA-500 NMR spectrometer was used to record ^1H, ^{13}C, ^{19}F NMR spectra at ambient temperature. ^1H chemical shifts were referenced to residual solvent. Temperature calibration of the NMR probe was accomplished using an anhydrous methanol standard. Line shape analysis of experimental NMR was performed using the Varian 6.1c software package. GC-MS data was obtained by injecting a dichloromethane solution into a Agilent 6890 GC equipped with an Agilent 5973 mass selective detector (EI). High-resolution EI mass spectroscopy was carried out by the Caltech Chemistry Mass Spectral Facility using a JEOL JMS600. UV-vis measurements were taken on a Cary 500 UV/Vis/NIR Spectrophotometer using a 0.1 cm quartz cell with a Teflon stopper. IR measurements were obtained with a KBr solution cell using a Bio-Rad Excalibur FTS 3000 spectrometer controlled by Bio-Rad Merlin Software (v.

2.97) set at 4 cm^{-1} resolution. X-ray diffraction studies were carried out in the Beckman Institute Crystallographic Facility on a Bruker Smart 1000 CCD diffractometer. Table II.1 shows X-ray diffraction data for **2.2**, **2.3**, and **2.4**.

Table II.1: X-ray diffraction data for **2.2**, **2.3**, and **2.4**.[a]

	2.2	**2.3**	**2.4**
Chemical Formula	$C_{40}H_{52}CuN_2S_4$	$C_{72}H_{64}BCu_2F_{24}N_4S_4 \cdot ½ (C_4H_{10}O)$	$C_{20}H_{26}ClCuNS_2$
Formula Weight	816.206	1716.478	443.53
T (K)	98	100	96
λ (Å)	0.71073	0.71073	0.71073
a (Å)	10.2263(9)	10.3179(8)	17.0807(13)
b (Å)	10.6226(9)	19.3779(14)	12.3173(10)
c (Å)	19.4884(17)	19.9116(15)	19.5782(15)
α (º)	94.017(2)	74.234(1)	90
β (º)	90.634(2)	83.222(1)	90
γ (º)	107.305(1)	85.603(1)	90
V ($Å^3$)	2015.1(3)	3800.4(5)	4119.0(6)
Space Group	P-1 (#2)	P-1 (#2)	Pbca (#61)
Z	2	2	8
D_{calcd} (g/cm^3)	1.345	1.500	1.430
μ (mm^{-1})	1.292	0.773	1.396
R1, wR2 (I>2σ(I))	0.0303, 0.0660	0.0393, 0.0810	0.0381, 0.0694

[a] $R1 = \Sigma ||F_o|-|F_c|| / \Sigma |F_o|$, $wR2 = \{\Sigma[w(F_o^2-F_c^2)^2]/\Sigma[w(F_o^2)^2]\}^{1/2}$

Magnetic Measurements. Measurements were recorded using a Quantum Designs SQUID magnetometer running MPMSR2 software (Magnetic Property Measurement System Revision 2). Data were recorded at 5000 G. Samples were suspended in the magnetometer in a clear plastic straw sealed under nitrogen with Lilly No. 4 gel caps. Loaded samples were centered within the magnetometer using the DC centering scan at 35 K and 5000 G. Data were acquired at 2 – 20 K (one data point every 2 K) and 20 – 295 K (one data point every 5 K). The magnetic susceptibility was adjusted for diamagnetic contributions using the constitutive corrections of Pascal's constants. The

molar magnetic susceptibility (χ_m) was calculated by converting the calculated magnetic susceptibility (χ) obtained from the magnetometer to a molar susceptibility (using the multiplication factor {(molecular weight) / [sample weight)*(field strength)]}). Curie-Weiss behavior was verified by a plot of χ_m^{-1} versus T. Graph II.2 shows the plot of the values for χT vs. T. Effective magnetic moments were calculated using equation 2.2.

$$\mu_{eff} = \text{sqrt}(7.997\ \chi_m\ T) \quad \text{(eq 2.2)}$$

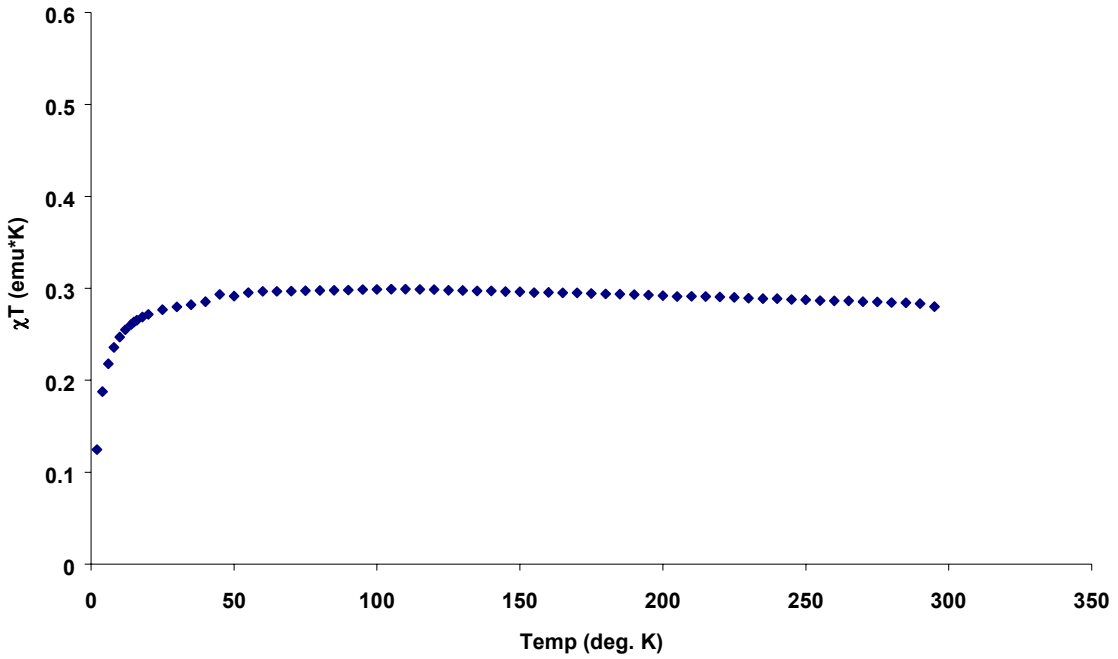

Graph II.2: SQUID Magnetization study of **2.3**.

EPR Measurements. X-band EPR spectra were obtained on a Bruker EMX spectrometer (controlled by Bruker Win EPR Software v. 3.0) equipped with a rectangular cavity working in the TE_{102} mode. Variable temperature measurements were conducted with an Oxford continuous-flow helium cryostat (temperature range 3.6 – 300 K). Accurate frequency values were provided by a frequency counter built into the microwave bridge. Solution spectra were acquired in toluene. Sample preparation was performed under a dinitrogen atmosphere in an EPR tube equipped with a ground glass joint.

Electrochemistry. Electrochemical measurements were carried out in a glove-box under a dinitrogen atmosphere in a one-compartment cell using a BAS model 100/W electrochemical analyzer. A glassy carbon electrode and platinum wire were used as the working and auxiliary electrodes, respectively. The reference electrode was $Ag/AgNO_3$ in THF. Solutions (CH_2Cl_2) of electrolyte (0.30 M tetra-*n*-butylammonium hexafluorophosphate) and analyte were prepared in a glove-box.

Electron self-exchange rate between 2.2 and 2.3: ^{1}H NMR spectra were acquired in CD_2Cl_2 on a Varian Inova Spectrometer operating at 499.852 MHz at 303 K. The data collection parameters were as follows: 0 s relaxation delay, 5.5 μs pulse width, and an 89988.8 Hz sweep width. The samples were weighed and dissolved in 1.0 mL of CD_2Cl_2, after which each sample tube was charged with ~0.5 mL of the solution. The sample concentrations, mole fractions, and experimental values for W are shown in Table II.2 below. The chemical shifts and line widths of the experimental spectra were obtained by Lorentzian line-fitting using the Varian 6.1c software package.

Table II.2. Line-broadening data, concentrations, and mole fractions used to estimate the lower boundary of the self-exchange reaction rate between **2.2** and **2.3** in dichloromethane solution. See Graph II.1 for plots of (i) chemical shift versus mole fraction of **2.2**, and (ii) W_2, W_3, and W_{23} versus χ_2.

	2.2 only	**2.3** only	Mix-A	Mix-B	Mix-C
$\chi_{2.2}$	1	0	0.75 ± 0.01	0.59 ± 0.01	0.41 ± 0.01
$\chi_{2.3}$	0	1	0.25 ± 0.01	0.41 ± 0.01	0.59 ± 0.01
Total conc. (mM)	-	-	29	24	27
Number of scans	100	1000	1000	1000	1000
Chemical shift (Hz)	619	3396	1314	1766	2263
W (Hz)	1.3 ± 0.2	807 ± 25	197 ± 15	314 ± 15	458 ± 15

Synthesis of 2-*tert*-butylsulfanyl bromobenzene. In air, 2-bromothiophenol (25 mL, 0.208 mol) was added dropwise to a vigorously stirred solution of *tert*-butyl alcohol (23 g, 0.312 mol), H_2O (150 mL), and concentrated H_2SO_4 (200 ml) at -10ºC in air. Following the addition, the reaction was allowed to come to ambient temperature and stirring was continued for 18 h, at which time ether (50mL) was added to the reaction mixture and the organic phase was washed with 1M Na_2CO_3 solution (100 mL), water (3 x 100 mL), dried over Na_2SO_4, and the solvent removed in vacuo. The resultant cloudy oil was fractionally distilled (90ºC/0.01 mmHg) affording a colorless oil.

^{1}H NMR (300 MHz, $CDCl_3$): δ 7.64 (m, 2H, Ar-*H*), 7.24 (t, 1H, Ar-*H*), 7.15 (t, 1H, Ar-*H*), 1.32 (s, 9 H, C(C*H*$_3$)$_3$). ^{13}C NMR (126 MHz, $CDCl_3$): δ 139.7, 134.4, 133.7, 132.8, 130.3, 127.5, 48.8, 31.5. GC-MS(M/z): 246/244[M], 190/188[M-(CH_3CCH_2)], 108, 109, 82, 69, 57.

Synthesis of bis(2-*tert*-butylsulfanylphenyl)amine: A 200 mL reaction vessel equipped with a Teflon stopcock and stir bar was charged with $Pd_2(dba)_3$ (0.365 g, 0.399 mmol), bis(diphenylphosphino)ferrocene (DPPF) (0.442 g, 0.798 mmol), and toluene (30 mL) under a dinitrogen atmosphere. The resulting solution was allowed to stir for 5 min, after which time 2-*tert*-butylsulfanyl bromobenzene (9.77 g, 39.9 mmol), 2-*tert*-butylsulfanyl aniline (7.23 g, 39.9 mmol), and additional toluene (70 mL) were added. The subsequent addition of NaO^tBu (5.37 g, 55.9 mmol) resulted in a brown solution that was stirred vigorously for 18 h at 100 °C. The solution was then allowed to cool and filtered through a silica plug that was then extracted with toluene to ensure complete removal of the desired product. Concentration of the collected extracts and removal of solvent yielded a

brown solid. These solid were extracted with hexanes and filtered. Purification by recrystallization from hexanes at –30 ºC afforded beige crystalline blocks (11.95 g, 87%). ^{1}H NMR (300 MHz, CD_2Cl_2): δ 8.30 (s, 1H, N-*H*), 7.52 (d, 2H, Ar-*H*), 7.43 (d, 2H, Ar-*H*), 7.25 (t, 2H, Ar-*H*), 6.83 (t, 2H, Ar-*H*), 1.33 (s, 18 H, C(C*H*$_3$)$_3$). ^{13}C NMR (126 MHz, $CDCl_3$): δ 145.8, 140.0, 130.2, 120.5, 120.0, 115.4, 47.9, 31.3. IR (KBr/CH_2Cl_2, cm^{-1}): 2924, 1575, 1509, 1364, 1319, 1167, 1034. HR-EI MS: Calcd for $C_{20}H_{27}NS_2$: 345.1585; Found: 345.1575.

Synthesis of [Li][SNS], 2.1: In a 250 mL flask, bis(2-*tert*-butylsulfanylphenyl)amine (2.5 g, 7.25 mmol) was dissolved in petroleum ether (100 mL) and a 1.6 M solution of *n*-butyl lithium in hexanes (5.9 mL, 9.43 mmol) was added dropwise with stirring at ambient temperature. A pale yellow solid began precipitating immediately and stirring was continued for 20 min. The solids were collected on a sintered glass frit and washed with petroleum ether (3 x 30mL). A spectroscopically pure off-white powder (2.5 g, 98%) was obtained upon drying in vacuo.

^{1}H NMR (300 MHz, C_6D_6): δ 7.52 (d, 2H, Ar-*H*), 7.34 (d, 2H, Ar-*H*), 7.15 (t, 2H, Ar-*H*), 6.68 (t, 2H, Ar-*H*), 1.11 (s, 18 H, C(C*H*$_3$)$_3$). ^{13}C NMR (126 MHz, C_6D_6): δ 164.7, 139.5, 131.0, 123.7, 121.7, 117.3, 47.4, 31.5.

Synthesis of {[SNS]Cu}$_2$, 2.2: A solution of **2.1** (800 mg, 2.28 mmol) in benzene (20 mL) was added dropwise with stirring to a suspension of CuBr·Me_2S (469 mg, 2.28 mmol) in benzene (40 mL). The solution immediately became bright yellow in color and after 4 h the reaction mixture was filtered through a pad of Celite on a sintered glass frit and the solvent removed in vacuo. The yellow solids were washed with petroleum ether (3x50 mL) and dried thoroughly which afforded spectroscopically pure product (850 mg,

91%). This complex decomposes photolytically over time so efforts were made to minimize light exposure during synthesis and storage. Analytically pure product is obtained as fine yellow crystalline needles by cooling a methylene chloride solution at -35 ºC.

^{1}H NMR (300 MHz, CD_2Cl_2): δ 7.32 (d, 2H, Ar-*H*), 7.06 (t, 2H, Ar-*H*), 6.91 (d, 2H, Ar-*H*), 6.57 (t, 2H, Ar-*H*), 1.23 (s, 18 H, C(CH_3)$_3$). ^{13}C NMR (126 MHz, CD_2Cl_2): δ 160.8, 136.3, 130.3, 122.9, 121.4, 116.3, 49.8, 31.1. UV/Vis/NIR (CD_2Cl_2, nm ($M^{-1}cm^{-1}$)): 426 (4000). IR (KBr pellet, cm^{-1}): 3045 (w), 2959 (m), 2921 (w), 1573 (s), 1543 (m), 1451 (s), 1428 (s), 1362 (m), 1312 (s), 1268 (m), 1154 (s), 1123 (w), 1031 (m), 818 (w), 743 (s), 725 (m). Anal. Calcd. for $C_{40}H_{52}Cu_2N_2S_4$: C, 58.86; H, 6.42; N, 3.43. Found: C, 58.46; H, 6.22; N, 3.28.

Synthesis of [{(SNS)Cu}$_2$][B($C_6H_3(CF_3)_2)_4$], 2.3: In a 20 mL reaction vessel equipped with a Teflon stirbar, **2.2** (150.0 mg, 0.184 mmol) was suspended in diethyl ether (15 mL) and [Cp_2Fe][B(3,5-$(CF_3)_2C_6H_3)_4$] (192.8 mg, 0.184 mmol) was added as a solid in one portion. The green reaction mixture gradually became red-brown in color and after 90 min, the solution was filtered through glass wool, and the filtrate was dried in vacuo. The solids were extracted with petroleum ether (3 x 30 mL) to remove the ferrocene byproduct, and drying under reduced pressure afforded the desired product as a burgundy solid (290 mg, 94%). Analytically pure material was obtained by recrystallization from layering a diethylether solution with petroleum ether.

^{19}F NMR (282 MHz, CD_2Cl_2): -60.19 (s, Ar-CF_3). IR (KBr pellet, cm^{-1}): 3293 (w), 3053 (w), 2968 (m), 1609 (m), 1578 (m), 1499, (m), 1454 (s), 1355 (s), 1279 (s), 1133 (br s), 887 (m), 835, (m), 756 (m), 756 (m), 714 (m), 670 (m). UV/Vis/NIR(CD_2Cl_2, nm (M^{-}

$^{1}cm^{-1}$)): 426(2500), 527(1650), 716(590), 1165(2050), 1920(4800). SQUID (solid, average 10-295 K): 1.52 B.M. (R^2 = 0.9991). Anal. Calcd. for $C_{72}H_{64}BCu_2F_{24}N_2S_4$: C, 51.49; H, 3.84; N, 1.67. Found: C, 51.63; H, 3.80; N, 2.00.

Synthesis of (SNS)CuCl, 2.4: In a 50 ml round bottom flask equipped with a Teflon stirbar, CuCl·0.66 THF (1.00 g, 5.50 mmol), was suspended in THF (30 mL) and **2.2** (1.93 g, 5.50 mmol) was added portionwise immediately affording a forest-green solution. The reaction mixture was stirred for 18 h at ambient temperature and the solvent was removed in vacuo. The resultant solid was triturated with benzene (2 x 10 mL), extracted into benzene, filtered through Celite and dried thoroughly under reduced pressure to afford **2.4** (2.30 g, 94%). Analytically pure material was obtained by recrystallization from THF/petroleum ether solution at -30 ºC.

IR (KBr pellet, cm^{-1}): 3056 (w), 2961 (w), 1573, (m), 1456 (s), 1431 (m), 1365 (m), 1321 (s), 1240 (w), 1155 (m), 1032 (w), 767 (w), 750 (m), 740 (m). UV/Vis/NIR (CD_2Cl_2, nm ($M^{-1}cm^{-1}$)): 606 (600), 1280 (280). Anal. Calcd. for $C_{20}H_{26}ClCuNS_2$: C, 54.16; H, 5.91; N, 3.16. Found: C, 54.22; H, 5.84; N, 3.08.

Reduction of 2.4 to 2.2: An amalgam of sodium (14.3 mg, 0.622 mmol) in mercury (11.1 g, 55.3 mmol) was prepared in a 20 mL reaction vessel and a solution of **2.4** (263 mg, 0.592 mmol) in THF (10 mL) was added. The reaction mixture was vigorously stirred for 6 h, filtered through Celite, and dried in vacuo. The yellow solid was extracted into benzene (20 ml), lyophilized, and washed with cold petroleum ether to afford spectroscopically pure **2.2** (188 mg, 78%).

II.D. References Cited

[1] (a) Guss, J. M.; Freeman, H. C. *J. Mol. Biol*. **1983**, *169*, 521. (b) Gray, H. B.; Malmstrom, B. G.; Williams, R. J. P. *J. Biol. Inorg. Chem*. **2000**, *5*, 551.

[2] Shibata, N.; Inoue, T.; Nagano, C.; Nishio, N.; Kohzuma, T.; Onodera, K.; Yoshizaki, F.; Sugimura, Y.; Kai, Y. *J. Biol. Chem*. **1999**, *274*, 4225.

[3] Suzuki, S.; Kataoka, K.; Yamaguchi, K.; Inoue, T.; Kai, Y. *Coord. Chem. Rev*. **1999**, *192*, 245.

[4] (a) Ambundo, E. A.; Yu, Q.; Ochrymowycz, L. A.; Rorabacher, D. B. *Inorg. Chem*. **2003**, *42*, 5267. (b) Kyritsis, P.; Dennison, C.; Ingeldew, W. J.; McFarlane, W.; Sykes, A. G. *Inorg. Chem*. **1995**, *34*, 5370. (c) Groenveld, C. M.; Canters, G. W. *J. Biol. Chem*. **1988**, *263*, 167. (d) Groenveld, C. M.; Dahlin, S.; Reinhammer, B.; Canters, G. W. *J. Am. Chem. Soc*. **1987**, *109*, 3247.

[5] (a) Solomon, E. I.; LaCroix, L. B.; Randall, D. W. *Pure Appl. Chem*. **1998**, *70*, 799. (b) Randall, D. W.; Gamelin, D. R.; LaCroix, L. B.; Solomon, E. I. *J. Biol. Inorg. Chem*. **2000**, *5*, 16.

[6] Marcus, R. A.; Sutin, N. *Biochim. Biophys. Acta* **1985**, *811*, 265.

[7] (a) Ferguson-Miller, S.; Babcock, G. T. *Chem. Rev*. **1996**, *96*, 2889. (b) Gamelin, D. R.; Randall, D. W.; Hay, M. T.; Houser, R. P.; Mulder, T. C.; Canters, G. W.; de Vries, S.; Tolman, W. B.; Lu, Y.; Solomon, E. I. *J. Am. Chem. Soc*. **1998**, *120*, 5246. (c) George, S. D.; Metz, M.; Szilagyi, R. K.; Wang, H. X.; Cramer, S. P.; Lu, Y.; Tolman, W. B.; Hedman, B.; Hodgson, K. O.; Solomon, E. I. *J. Am. Chem. Soc.* **2001**, *123*, 5757. (d) Ramirez, B. E.; Malmstrom, B. G.; Winkler, J. R.; Gray, H. B. *Proc. Natl. Acad. Sci. U.S.A*. **1995**, *92*, 11949.

[8] (a) Kroneck, P. M. H.; Antholine, W. E.; Riester, J.; Zumft, W. G. *FEBS Lett.* **1989**, *248*, 212. (b) Kroneck, P. M. H.; Antholine, W. E.; Riester, J.; Zumft, W. G. *FEBS Lett.* **1988**, *242*, 70. (c) Antholine, W. E.; Kastrau, D. H. W.; Steffens, G. C. M.; Buse, G.; Sumft, W. G.; Kroneck, P. M. H. *Eur. J. Biochem*. **1992**, *209*, 875.

[9] (a) Houser, R. P.; Young, Jr., V. G.; Tolman, W. B. *J. Am. Chem. Soc.*, **1996**, *118*, 2101. (b) Blackburn, N. J.; deVries, S.; Barr, M. E.; Houser, R. P.; Tolman, W. B.; Sanders, D.; Fee, J. A. *J. Am. Chem. Soc*. **1997**, *119*, 6135. (c) Hagadorn, J. R.; Zahn, T. I.; Que Jr., L.; Tolman, W. B. *J. C. S. Dalton Trans.* **2003**, 1790.

[10] Al-Obaidi, A.; Baranovič, G.; Coyle, J.; Coates, C. G.; McGarvey, J. J.; McKee, V.; Nelson, J. *Inorg. Chem.* **1998**, *37*, 3567.

[11] (a) LeCloux, D. D.; Davydov, R.; Lippard, S. J. *Inorg. Chem*. **1998**, *37*, 6814. (b) LeCloux, D. D.; Davydov, R.; Lippard, S. J. *J. Am. Chem. Soc*. **1998**, *120*, 6810. (c) He, C.; Lippard, S. J. *Inorg. Chem.* **2000**, *39*, 5225.

[12] Gupta, R.; Zhang, Z. H.; Powell, D.; Hendrich, M. P., Borovik, A. S. *Inorg. Chem.*, **2002**, *41*, 5100.

[13] (a) Nelson J.; McKee, V.; Morgan, G. G. *Prog. Inorg. Chem*. **1998**, *47*, 167. (b) Coyle, J. L.; Elias, H.; Herlinger, E.; Lange, J.; Nelson, J. *J. Biol. Inorg. Chem*. **2001**, *6*, 285.

[14] Dicopper systems structurally distinct from the Cu_2X_2 diamond core motif have in certain cases shown a reversible $Cu^1Cu^1/Cu^{1.5}Cu^{1.5}$ redox process. See, for example, 11c and references therein.

[15] (a) Blackburn, N. J.; Barr, M. E.; Woodruff, W. H.; van der Oost, J.; de Vries, S. *Biochemistry* **1994**, *33*, 10401. (b) Williams, M.; Lapplalainen, P.; Kelly, M.; Sauer-Eriksson, E.; Saraste, M. *Proc. Natl. Acad. Sci. U.S.A*. **1995**, *92*, 11955.

[16] See related L_2N^- ligand [bis(8-quinolinyl)amido]Li: Peters, J. C.; Harkins, S. B.; Brown, S. D.; Day, M.W. *Inorg. Chem*. **2001**, *40*, 5083.

[17] (a) Wolfe, J. P.; Tomori, H.; Sadighi, J. P.; Yin, J. J.; Buchwald, S. L. *J. Org. Chem.* **2000**, *65*, 1158. (b) Alcazar-Roman, L. M.; Hartwig, J. F.; Rheingold, A. L.; Liable-Sands, L. M.; Guzei, I. A. *J. Am. Chem. Soc.* **2000**, *122*, 4618.

[18] Puzas, J. P.; Nakon, R.; Petersen, J. L. *Inorg. Chem*. **1986**, *25*, 3837.

[19] Cambridge Structural Database; Cambridge University: Cambridge, England (accessed November 2003).

[20] Scaling of the $Cu^{1.5}Cu^{1.5}/Cu^{1}Cu^{1}$ redox couple to NHE provides an approximate value of +550 mV, reasonably close to the $Cu^{II}Cu^{I}/Cu^{I}Cu^{I}$ couple measured for the Cu_A cofactor of *Thermus thermophilus* cytochrome ba_3 in water (+240 mV).[33]

[21] The second oxidation process in dichloromethane solvent suggests the process may be modestly reversible under such conditions.

[22] Geometry optimization and electronic structure calculation (JAGUAR 5.0, B3LYP/LACVP**) were performed on the complete structure of the cation of **3** assuming a doublet ground-state (no symmetry constraints applied; crystallographic coordinates of **3** were used as the HF initial guess). Jaguar 5.0, Schrodinger, LLC, Portland, Oregon, 2002.

[23] Xie, B.; Elder, T.; Wilson, L. J.; Stanbury, D. M. *Inorg. Chem*. **1999**, *38*, 12.

[24] (a) Jameson, D. L.; Anand, R. *J. Chem. Ed.* **2000**, *77*, 88. (b) Nielson, R. M.; McManis, G.; Golovin, M. N.; Weaver, M. J. *J. Phys. Chem.*, **1988**, *92*, 3441. (c) Yang, E. S.; Chan, M. S.; Wahl, A.C. *J. Phys. Chem.* **1980**, *84*, 3094. (d) Soper, J. D.; Mayer, J. M. *J. Am. Chem. Soc.* **2003**, *125*, 12217.

[25] Larsen, D. W.; Wahl, A. C. *J. Phys. Chem*. **1965**, *43*, 3765.

[26] Chan, M. S.; Deroos, J. B.; Wahl, A. C. *J. Phys. Chem*. **1973**, *77*, 2163.

[27] Slutter, C. E.; Langen, R.; Sanders, D.; Lawrence, S. M.; Wittung, P.; Di Bilio, A.; Hill, M. G.; Fee, J. A.; Richards, J. H.; Winkler, J. R.; Malmström, B. G. *Inorg. Chim. Acta* **1996**, *243*, 141.

[28] Lappalainen, P.; Watmough, N. J.; Greenwood, C.; Saraste, M. *Biochemistry* **1995**, *34*, 5824.

[29] Jensen, M. R.; Hansen, D. F.; Led, J. J. *J. Am. Chem. Soc.* **2002**, *124*, 4093.

[30] Courtin, v. A.; von Tobel, H. R.; Auerbach, G. *Helv. Chim. Acta*. **1980**, *63*, 1412.

[31] Chåvez, I.; et. al. *J. Organomet. Chem*. **2000**, *601*, 126.

[32] So, J. H.; Boudjouk, P. *Inorg. Chem*. **1990**, *29*, 1592. The precise number of equivalents of THF contained in this starting material was determined by microanalysis.

[33] Immoos, C.; Hill, M. G.; Sanders, D.; Fee, J. A.; Slutter, C. E.; Richards, J. H.; Gray, H. B. *J. Biol. Inorg. Chem*. **1996**, *1*, 529.

Chapter III

Luminescence Studies of Dicopper(I) Complexes Supported by Bis(2-diisobutylphoshinophenyl)amido Ligands †

†Adapted from Harkins, S. B.; Peters, J. C. *J. Am. Chem. Soc.* **2005**, *127*, 2030.

III.A. Introduction

Photoluminescent complexes have garnered much attention due to their possible utilization in electrochemical devices, as sensors and biological imaging agents, and in solar energy conversion schemes.[1] In this context, polypyridine-supported Cu(I) systems show promising features including the availability of low-lying charge-transfer (CT) excited states and the relatively low cost of copper in comparison to other transition metal luminophores. However, their tendency to display weak emission and short-lived excited states is problematic.[2] McMillin has underscored these collective points,[3] and his group recently reported a fascinating mononuclear complex, $[Cu(dmp)(POP)]^+$ (dmp = 2,9-dimethyl-1,10-phenanthroline; POP = bis[2-(diphenylphosphino)phenyl]ether), that exhibits both a relatively high quantum yield and long-lived excited-state as compared to other polypyridine-Cu(I) systems.[4] Incorporation of a bulky, bis(phosphine) chelate appears to create a rigid environment around the copper center which (i) suppresses solvent-induced exciplex formation, and (ii) limits problematic ligand dissociation from the excited state.

Herein we describe an amido-bridged bimetallic copper system, $\{(PNP)Cu^I\}_2$ (**3.2**), derived from a chelating bis(phosphine)amide ligand, Figure III.1 ((PNP) = bis(2-(diisobutylphosphino)phenyl)amide). This species is an exceptional luminophore in its own right. Aside from the absence of supporting polypyridine ligands, its combined quantum yield ($\phi > 0.65$) and lifetime ($\tau > 10$ μs), in combination with its dinuclear structure and redox behavior, are without precedent. The synthesis of **3.2** was motivated by our recent elucidation of the dinuclear, thioether-supported Cu_2N_2 complex $\{(SNS)Cu^I\}_2$ ($(SNS)^-$ = bis(2-*tert*-butylsulfanylphenyl)amide).[5] $\{(SNS)Cu^I\}_2$ exhibits a

reversible $1e^-$ oxidation to form a mixed-valence $[\{(SNS)Cu^{1.5}\}_2]^+$ complex, and electrochemical and XRD studies establish minimal structural reorganization between these two redox partners. While $\{(SNS)Cu^{I}\}_2$ is negligibly emissive at 298 K, its phosphine congener **3.2** emits strongly in solution and in the solid-state when irradiated by visible light.

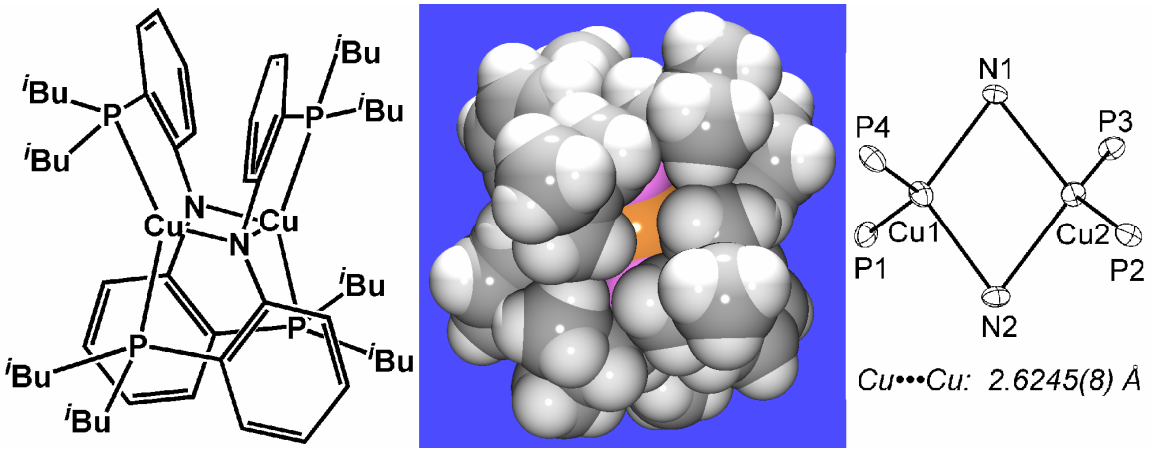

Figure III.1: *Left,* Molecular representation of **3.2**. *Center,* Space-filling representation of **3.2** from crystal coordinates. *Right*, Displacement ellipsoid representations (50%) of the core atoms of **3.2**.

III.B. Results and Discussion

The required tridentate PNP-H ligand, **3.1**, was synthesized by addition of ^{n}BuLi to bis(2,2'-difluorophenyl)amine in THF followed by the addition of lithium diisobutylphosphide.[6] Heating this mixture at 45 °C for 4 days and subsequent passage of the crude product through silica gel afforded amine **3.1** as a spectroscopically pure viscous oil (75% yield), Figure III.2. Deprotonation with ^{n}BuLi affords [PNP][Li], $\{[\mathbf{3.1}]Li\}_2$, in good yield. Related bis(phosphino)amido ligands were first introduced by Fryzuk and have received the attention of several groups more recently.[7,8] $\{[\mathbf{3.1}]Li\}_2$ reacts rapidly with $CuBr{\cdot}Me_2S$ in diethyl ether to generate a luminescent yellow solution.

The neutral, diamagnetic copper complex **3.2** can be subsequently isolated in pure form by crystallization (92%). Alternatively, complex **3.2** can be generated in good yield by the addition of $\{(2,4,6\text{-}Me_3C_6H_2)Cu\}$[9] to free amine **3.1**, producing mesitylene upon metallation.

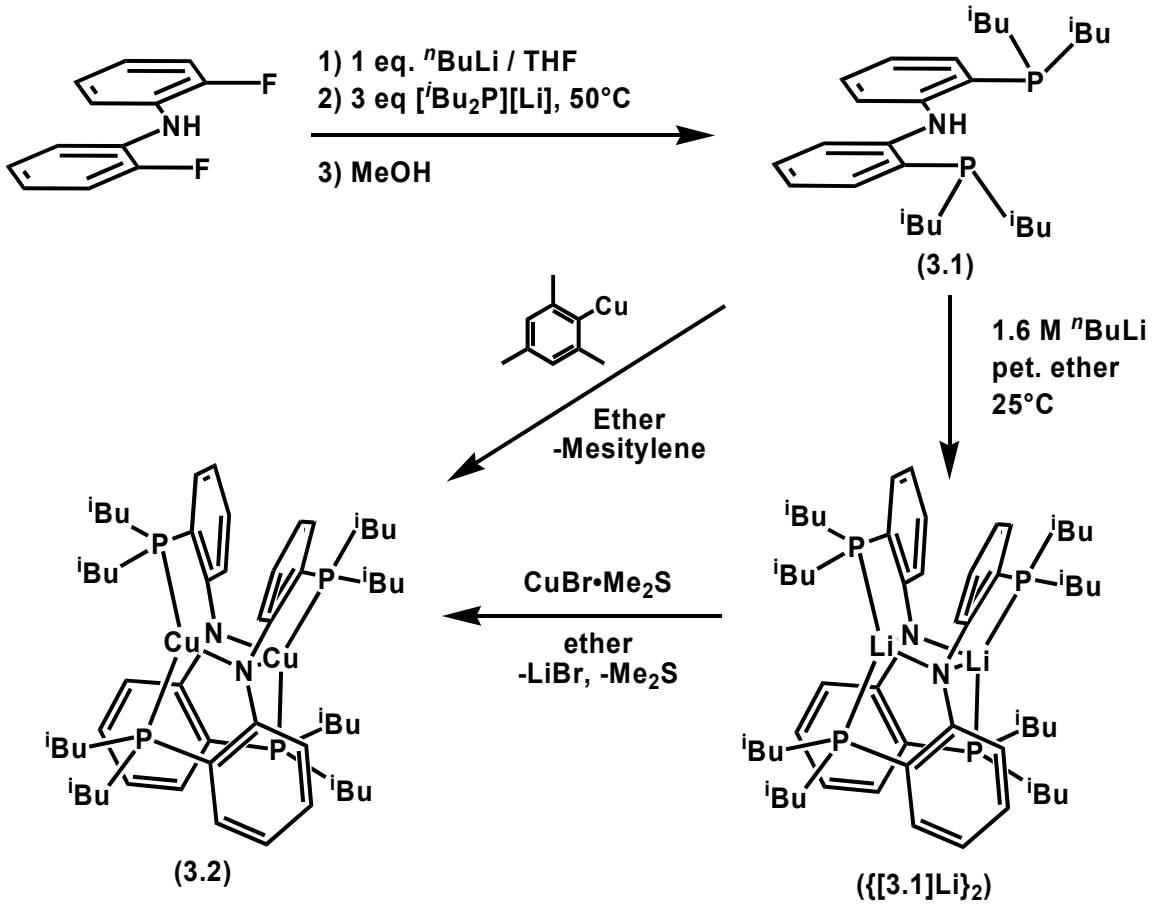

Figure III.2: Synthesis of **3.1**, **{[3.1][Li]}$_2$**, and **3.2**.

Complex **3.2** is characterized by a single resonance in its ^{31}P NMR spectrum (−33.9 ppm) and XRD analysis establishes the dimeric structure represented in Figure III.1. A short Cu···Cu bond distance of 2.6245(8) Å is observed that is similar in length to the Cu···Cu distance reported for $\{(SNS)Cu^{I}\}_2$. The P-Cu-P angles of 132.93(5)º and 137.69(5)º are significantly smaller than the S-Cu-S angles in $\{(SNS)Cu^{I}\}_2$ (avg 153º).

As a result the copper centers are less severely distorted from a tetrahedral geometry than in $\{(SNS)Cu^{I}\}_2$, which more closely approximates a cis-divacant octahedron at each copper site. These geometrical differences presumably arise from the different steric requirements of the thioether $[SNS]^-$ and diisobutylphosphine $[PNP]^-$ ligands.

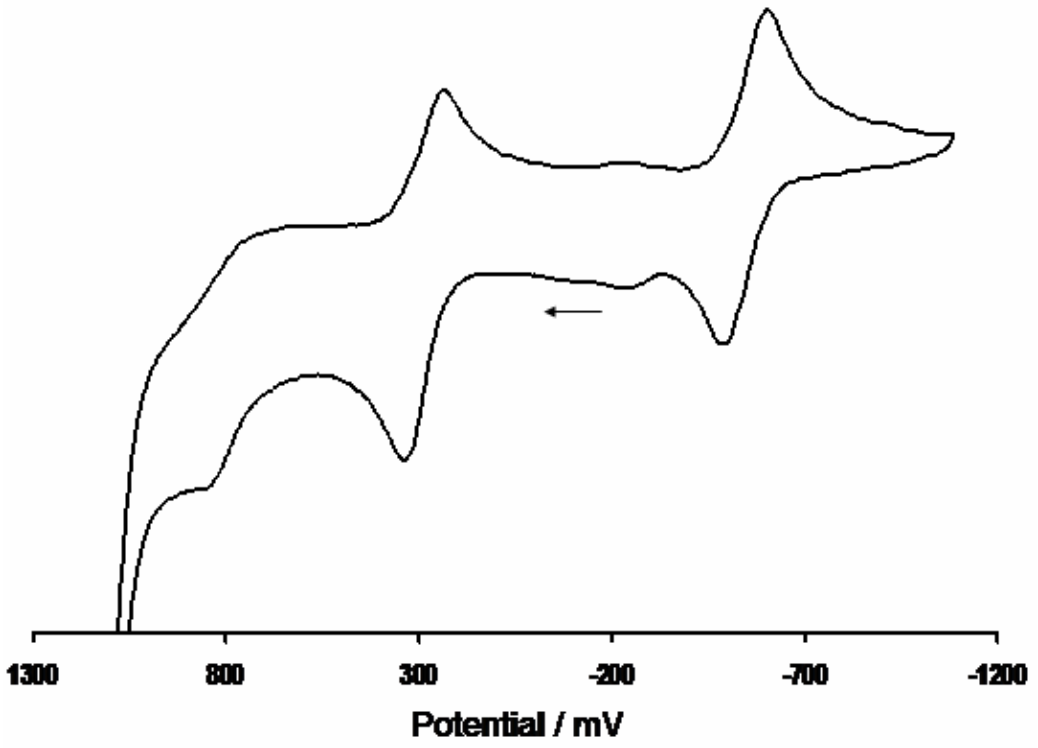

Figure III.3: Cyclic voltammetry of **3.2** referenced vs. Fc^+/Fc in CH_2Cl_2 (0.10 M $[^nBu_4N][PF_6]$, 250 mV/sec).

Electrochemical analysis of **3.2** in CH_2Cl_2 (Fc^+/Fc, 0.3 M $[^nBu_4N][PF_6]$, 250 mV/sec, Fc = ferrocene) reveals two reversible waves, one centered at −550 mV and the other at 300 mV, Figure III.3. An irreversible wave is encountered at higher potential (E_{pa} = 860 mV).[10] The event at −550 mV is assigned to a reversible $Cu^{1.5}Cu^{1.5}/Cu^{I}Cu^{I}$ redox process by analogy to the $\{(SNS)Cu^{I}\}_2$ system. The $Cu^{1.5}Cu^{1.5}/Cu^{I}Cu^{I}$ event is cathodically shifted for **3.2** in comparison to $\{(SNS)Cu^{I}\}_2$ (by ~ 160 mV) due to its stronger

phosphine donors. The second *reversible* wave observed for **3.2** ($E_{½}$ = 300 mV) is noteworthy and is distinct from $\{(SNS)Cu^{I}\}_2$, for which only an *irreversible* redox process is observed at similar potential (E_{pa}= 560 mV). Incorporation of the phosphine donors appears to stabilize an unusual second oxidation event in **3.2**, at least on the time scale of the electrochemical experiment (250 mV/s). While it is tempting to assign this second wave to a $Cu^{II}Cu^{II}/Cu^{1.5}Cu^{1.5}$ redox process, at this stage it is equally plausible to suggest that a ligand-centered oxidation process is operative.[11,12]

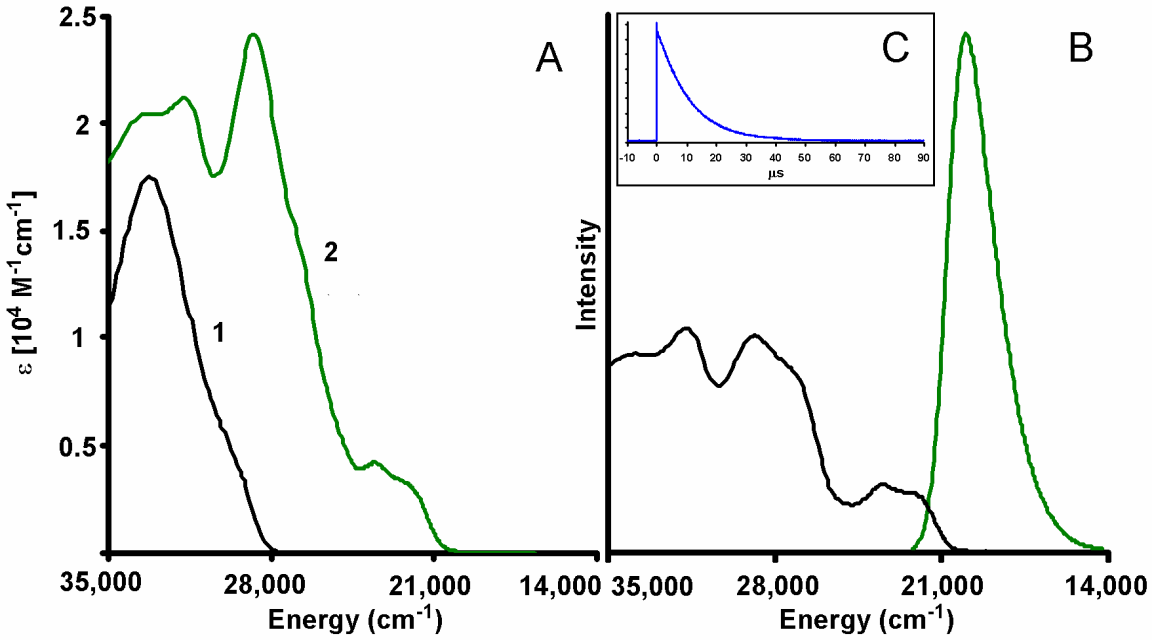

Figure III.4: *Left* (A): Absorption spectra for **3.1** and **3.2** in cyclohexane. *Right* (B): Corrected emission spectrum (green, λ_{ex} = 440 nm) and excitation spectrum (black, λ_{em} = 560 nm) of **3.2** in cyclohexane. *Inset* (C): Luminescence decay measurement of **3.2** in cyclohexane (laser pulse at t = 0 µs, λ_{ex} = 440 nm, λ_{em} = 510 nm).

The absorption spectra for ligand **3.1** and complex **3.2** are shown in Figure III.4(A), and the corrected emission and excitation spectrum for **3.2** (298 K in cyclohexane) is also shown (B).[13] The optical spectrum of **3.2** is typical for Cu(I). MLCT bands at 23,800 and

22,300 cm^{-1} give rise to its yellow color. Its emission spectrum, collected by excitation into its lowest energy absorption band (λ_{ex} = 440 nm, ≈ 22,700 cm^{-1}), shows a λ_{max} at 20,000 cm^{-1}. Its corresponding excitation profile is also shown (λ_{em} = 560 nm, ≈17,900 cm^{-1}). Low temperature emission studies at 77 K of **3.2** were also attempted for a frozen methylcyclohexane glass and on a single crystal of **3.2** under He, Figure III.5. While some enhanced vibrational structure was observed by going to lower temperature, no conclusions regarding the nature of the excited state could be reached. Interestingly, a high energy emission band at 480 nm was found in the sample of **3.2** in a methylcyclohexane glass, but not for those measurements done on the single crystal.

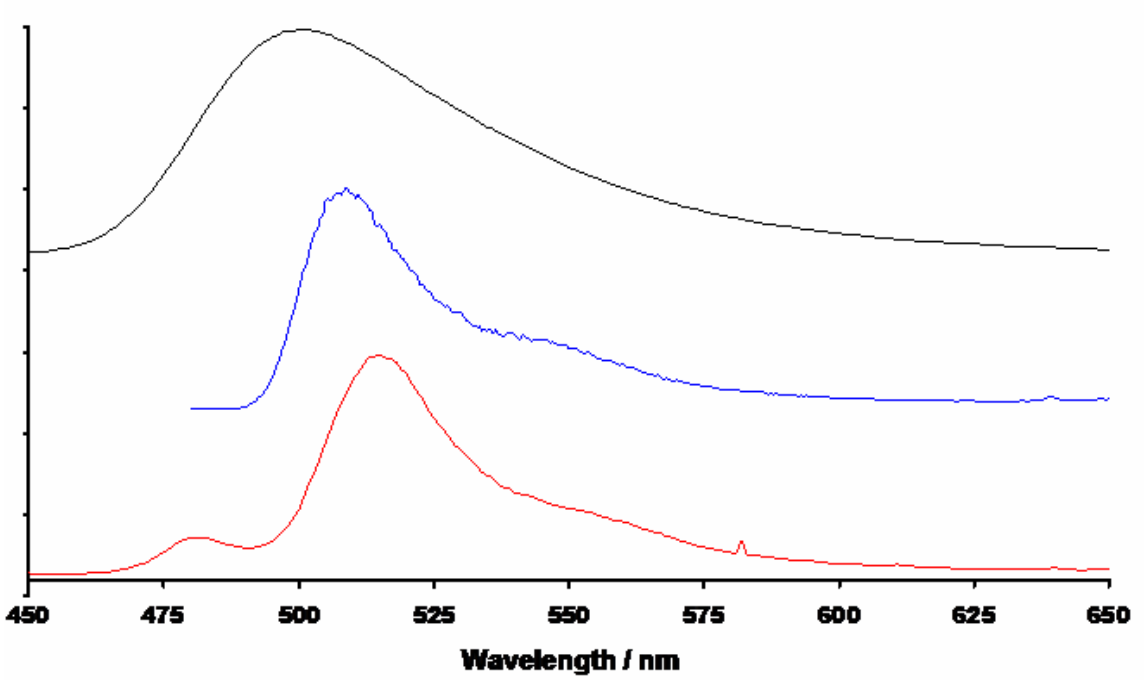

Figure III.5: Low temperature emission of **3.2**. *Black*: solution of 3.2 in cyclohexane (298 K); *Blue*: single crystal of **3.2** under $He_{(g)}$ (77 K); *Red*: frozen glass solution of **3.2** in methylcyclohexane (77 K).

The intensity of the emission from the excited state of **3.2**, ***3.2**, is quite striking to the eye, even at room temperature in relatively polar donor solvents such as tetrahydrofuran (THF). This property is consistent with the unusually high quantum yield

we measured for **3.2** at 298 K: $\phi = 0.68(2)$ in cyclohexane and $\phi = 0.67(4)$ in THF. These quantum yields were determined by established methods using a fluorescein standard ($\phi = 0.90$ in 0.1 N NaOH).[14] It was also of interest to determine the excited-state lifetime of ***3.2**, measured as 10.2(2) μs in cyclohexane (see inset in Figure III.4) and 10.9(4) μs in THF. These lifetimes were determined by a monoexponential fit to raw decay data collected at 510 nm upon excitation at 460 nm. Complex **3.2** is thus a remarkably efficient luminophore, with a lifetime similar to that McMillin has reported for mononuclear $[Cu(dmp)(POP)]^+$ and a quantum yield that is approximately four times greater. We also note that diffusion-limited excited state electron transfer ($k_Q = 1.2 \times 10^{10}$ $M^{-1}s^{-1}$) has been demonstrated by time-resolved quenching experiments using 2,6-dichloroquinone (Graph III.1).[15]

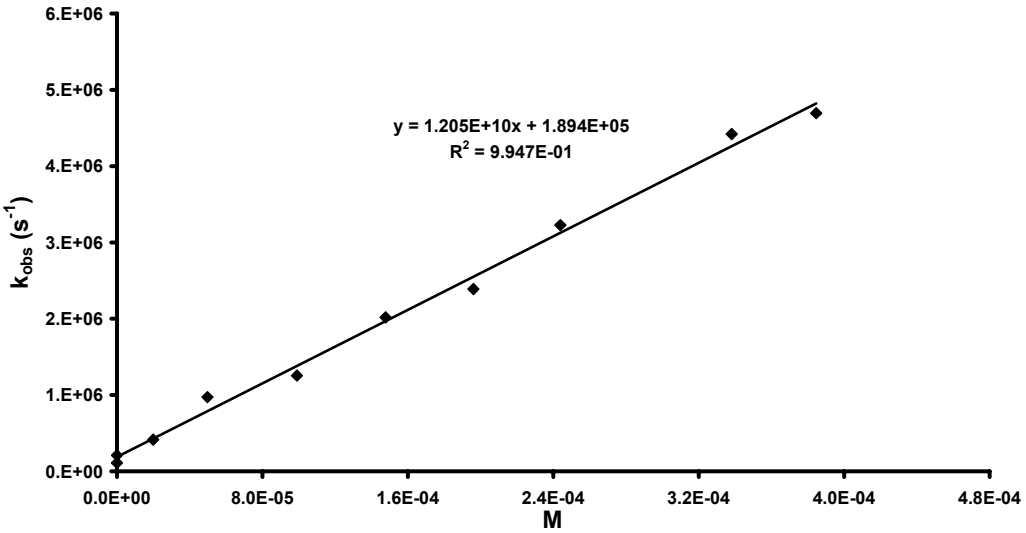

Graph III.1: Time-resolved emission quenching of **3.2** with DCQ in THF.

Emissive dinuclear copper systems have been reported previously, but these species typically feature much shorter excited-state lifetimes. Perhaps most structurally related to **3.2** is the neutral complex $\{[DPT]Cu^I\}_2$ (DPT = 1,3-triphenyltriazine anion), which features a Cu···Cu distance of 2.451(8) Å.[16] This neutral d^{10}-d^{10} system exhibits a

fluorescence maximum at 570 nm and a lifetime of only 2.23 ns at 77 K,[17a] approximately three orders of magnitude shorter than **3.2**. Other Cu^{I}_{2} luminophores that have been described are typically supported by polypyridine type ligands and have rather long Cu···Cu distances.[b] Quantum yields for these systems are small in magnitude by comparison to their well-studied, substituted $Cu(phen)_2^+$ analogues.[b]

The unusual emission properties exhibited by **3.2** may be due to several factors. Foremost among these may be the relatively low structural reorganization between **3.2** and ***3.2**. This assertion is at least consistent with the relatively narrow full-width at half-maximum of its emission band shown in Figure III.4 (B) (2400 cm^{-1}), which can be converted to an estimate of the total reorganization energy λ = 2600 cm^{-1}. Also, steric protection afforded by the bulky PNP ligand, in addition to the absence of a net cationic charge for **3.2**, removes the possibility of anion binding and likely renders the excited-state complex resistant to donor solvent ligation. Each of these factors can otherwise contribute to undesirable exciplex quenching. Lewis acidic Cu(I) cations, such as $Cu(phen)_2^+$ systems, suffer from exciplex quenching due to solvent and/or counter-anion binding in the excited state. The space-filling model of **3.2** shown in Figure III.1 reveals just how effectively the copper sites are shrouded by the surrounding phosphine ligand framework.

Table III.1 Comparison of bond lengths and angles between the determined by X-ray diffraction for **3.2** and those calculated by DFT.

Interatomic Distances (Å)	**X-ray**	**DFT**	**Interatomic Angles (deg.)**	**X-ray**	**DFT**
Cu1-Cu2	2.6245(8)	2.762	Cu1-N1-Cu2	75.10(12)	76.78
Cu1-N1	2.127(4)	2.208	Cu1-N2-Cu2	73.03(12)	73.98
Cu1-N2	2.191(4)	2.248	N1-Cu1-N2	107.20(14)	106.66
Cu2-N1	2.179(4)	2.239	N1-Cu2-N2	104.44(14)	102.56
Cu2-N2	2.219(4)	2.341			

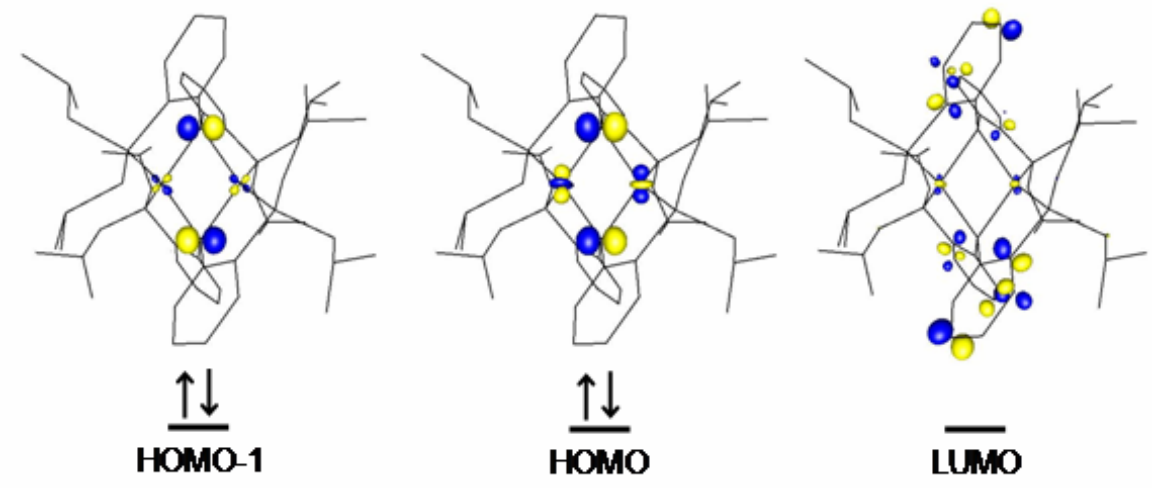

Figure III.6: Geometry optimization and electronic structure calculation for **3.2** using DFT (JAGUAR: B3LYP/LACVP**). Contour plot (value = 0.0905, 0.088, 0.065) of the highest lying molecular orbitals are shown.

A geometry optimization and electronic structure calculation of **3.2** using DFT (JAGUAR 5.0, B3LYP/LACVP**) was performed using the crystallographically determined X-ray coordinates as the initial guess for the geometry (Figure III.6).[18] The theoretically determined structure agrees well with that determined experimental by X-ray diffraction (Table III.1). The electronic structure of **3.2** afforded by the DFT calculation suggests that the redox active HOMO (Figure III.6) contains significant orbital contributions from the four atoms of the Cu_2N_2 diamond core. The HOMO is antibonding with respect to each of the four Cu-N interactions and also the Cu-Cu interaction. This orbital configuration is consistent with the $\{(SNS)Cu\}_2$ system (Chapter II). The LUMO is found to be virtually devoid of metal character and almost completely associated with the aryl ring structure. This result could indicate that the excited state involves promotion of an electron from the Cu_2N_2 core to the outer ligand framework.

As a final point of interest, we note that a value for E^{00} = 2.6 eV can be estimated from the intersection of the emission and excitation profiles of **3.2** (Figure III.7).

Subtracting this value from the reversible $Cu^{1.5}Cu^{1.5}/Cu^{1}Cu^{1}$ redox couple provides an estimated value of -3.2 V (vs. Fc^{+}/Fc) for the excited state reduction potential of ***3.2**. This estimated potential is unusually low, and it is possible that ***3.2** will prove to be a potent photoreductant/photosensitizer.[19] Indeed, given the presence of two reversible redox couples within this bimetallic copper system, there may be an opportunity to photochemically drive two-electron reaction processes.[20]

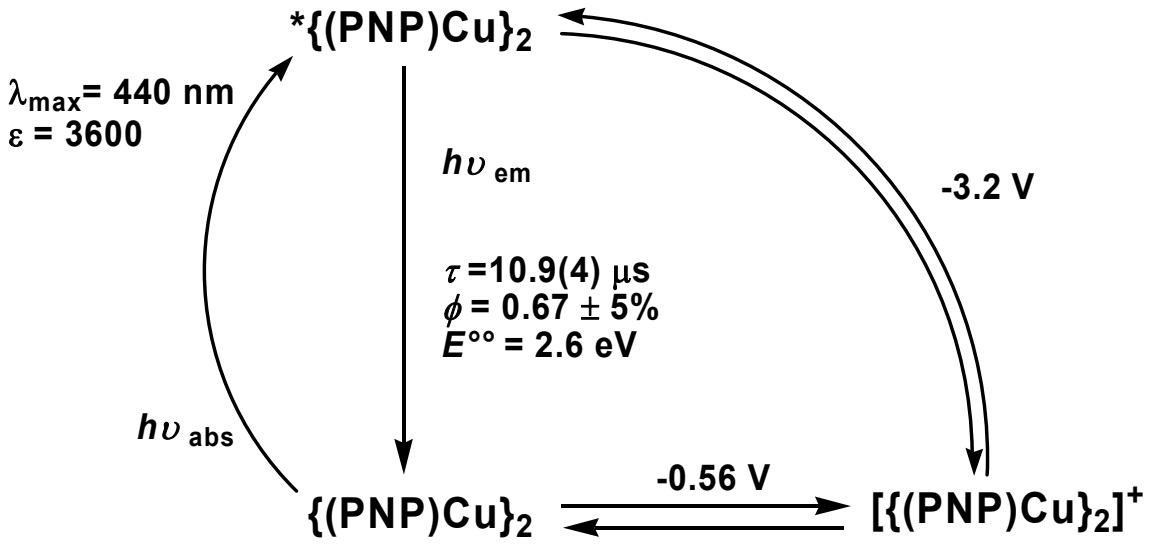

Figure III.7: Diagram of the photophysical and redox properties of **3.2**.

III.C. Experimental

General. All manipulations were carried out using standard Schlenk or glove-box techniques under a dinitrogen atmosphere. Unless otherwise noted, solvents were deoxygenated and dried by thorough sparging with N_2 gas followed by passage through an activated alumina column. Non-halogenated solvents were tested with a standard purple solution of sodium benzophenone ketyl in tetrahydrofuran in order to confirm effective oxygen and moisture removal. Spectral grade THF was purchased from Aldrich and distilled from molten potassium prior to use. All reagents were purchased from commercial vendors and used without further purification unless otherwise stated. A volumetric solution of 0.1 N NaOH was purchased from J. T. Baker and used as received. $[Cp_2Fe][B(C_6H_3(CF_3)_2)_4]$,[21] was prepared according to literature procedure. Elemental analyses were performed by Desert Analytics, Tucson, AZ. Deuterated solvents were purchased from Cambridge Isotope Laboratories, Inc., degassed, and dried over activated 3 Å molecular sieves prior to use. X-ray diffraction studies were carried out at the Beckman Institute Crystallographic Facility on a Brüker Smart 1000 CCD diffractometer and solved using SHELX v. 6.14.

Electrochemistry. Electrochemical measurements were carried out in a glove-box under a dinitrogen atmosphere in a one-compartment cell using a BAS model 100/W electrochemical analyzer. A glassy carbon electrode and platinum wire were used as the working and auxiliary electrodes, respectively. The reference electrode was $Ag/AgNO_3$ in THF. The ferrocene couple Fc^+/Fc was used as an external reference. Solutions (THF) of electrolyte (0.35 M tetra-*n*-butylammonium hexafluorophosphate) and analyte were also prepared under an inert atmosphere.

Spectroscopic measurements. High-resolution EI mass spectroscopy was carried out by the Caltech Chemistry Mass Spectral Facility using a JEOL JMS600. A Varian Mercury-300 or INOVA-500 NMR spectrometer was used to record ^{1}H, ^{13}C, ^{19}F, ^{31}P NMR spectra at ambient temperature. ^{1}H and ^{13}C chemical shifts were referenced to the residual solvent peaks. ^{19}F and ^{31}P NMR chemical shifts were referenced to external hexafluorobenzene (δ = -165 ppm) and phosphoric acid (δ = 0 ppm), respectively. Emission spectra were recorded on a Spex Fluorolog-2 spectro-fluorometer. Excitation for the luminescence lifetime experiments employed 8 ns pulses (at a repetition rate of 10 Hz) from a Nd:YAG laser pumped OPO (Quanta Ray Pro, Spectra Physics).. The luminescence was dispersed through a monochromator (Instruments SA DH-10) onto a photomultiplier tube (PMT) (Hamamatsu R928). The PMT current was amplified and recorded with a transient digitizer (Tektronix). UV-vis measurements were taken on a Cary 50 UV/Vis Spectrophotometer using a 1 cm quartz cell or 500 UV/Vis/NIR Spectrophotometer using either a 2 cm or 1 cm quartz cell sealed with a Teflon stopper.

Synthesis of Lithium Diisobutylphosphide. In a 500 mL Erlenmeyer flask diisobutylphosphine (25 g, 0.171 mol) was dissolved in 200 mL of petroleum ether and cooled to -80ºC, at which time at 1.6 M solution of ^{n}butyl lithium in hexane (107 mL, 0.171 mol) was added over 20 min. The reaction was then stirred at ambient temperature for 24 h, concentrated in vacuo to ca. 50 mL, and the white solids were then collected on a sintered-glass frit. Washing of the solids with petroleum ether afforded a single phosphorous containing product (21.1 g, 81%) as by ^{31}P NMR upon drying.

$^{31}P\{^{1}H\}$ NMR (121.5 MHz, THF): -91.2.

Synthesis of Bis(2-(diisobutylphosphino)phenyl)amine, 3.1. In a 250 mL sealable reaction bomb, a 1.6 M ^{n}butyl lithium solution (7.9 mL, 12.6 mmol) in hexanes was added dropwise to a solution of bis(2-fluorophenyl)amine (2.46 g, 12.0 mmol) in THF (20 mL). After stirring for 15 min, the solution was concentrated in vacuo to remove the majority of the reaction volatiles after which time a solution of lithium diisobutylphosphide (5.47 g, 36 mmol) in THF (40 mL) was added and the vessel was sealed with a Teflon plug. The reaction was heated at 45ºC for 4 days and was monitored by ^{19}F NMR for the complete disappearance of the aryl fluoride resonance. The reaction was then quenched with methanol (5 mL) and the solution became yellow in color. Petroleum ether (50 mL) was added and the mixture was filtered twice through Celite to remove solids. Removal of the solvent in vacuo afforded an orange oil which was diluted in petroleum ether (30 mL) and flashed through two plugs of silica gel in a 60 mL sintered-glass frit. Evaporation of the solvent under reduced pressure afforded a spectroscopically pure, pale green oil (4.10 g, 75%).

^{1}H NMR(300.1 MHz, $CDCl_3$): δ 8.03 (t, 1H), 7.52 (m, 2H), 7.33 (m, 2H), 7.26 (t, 2H), 7.00 (t, 2H), 1.73 (m, 12H), 1.08 (d, 12), 1.03 (d, 12H). ^{13}C{^{1}H} NMR(75.5 MHz, $CDCl_3$): δ 147.8, 131.8, 129.4, 128.0, 121.0, 119.3, 116.7, 39.4, 26.6, 24.7, 24.3. ^{31}P{^{1}H} NMR (121.5 MHz, $CDCl_3$): δ -54.5. UV-vis (benzene, nm($M^{-1}cm^{-1}$)): 302 (18,700), sh 334(5900). FAB+ MS: calcd for $C_{28}H_{45}NP_2$: 457.3027. Found: 458.3122 [M+H], 400.2226 [M-^{i}Bu], 312.1904 [M-($^{i}Bu_2P$)].

Synthesis of {[PNP]Li}$_2$, {[3.1]Li}$_2$. At ambient temperature a 1.6 M ^{n}butyl lithium solution (4.0 mL, 6.4 mmol) in hexanes was added dropwise to a solution of **3.1** (2.63 g, 5.76 mmol) in petroleum ether (50 mL) over 15 min. The reaction was stirred for 30 min,

at which time a solid began to precipitate. The solution was concentrated to ca. 30 mL and cooled to -30 °C for 12 h. The resultant solids were collected on a sintered-glass frit as fine pale yellow powder, dried thoroughly (2.24 g, 84 %).

^{1}H NMR(499.9 MHz, C_6D_6): δ 7.21 (m, 2 H), 7.06 (m, 4 H), 6.71 (m, 2 H), 1.8-0.6 (br m, 36 H). $^{13}C\{^{1}H\}$ NMR(125.7 MHz, C_6D_6): δ 170.6, 132.4, 131.2, 128.7, 128.1, 118.6, 42.3, 36.2, 26.3, 25.3. $^{31}P\{^{1}H\}$ NMR (121.5MHz, C_6D_6): δ -49.4 (q, 61 Hz). UV-vis (cyclohexane, nm($M^{-1}cm^{-1}$)): 301(18,700), 357(31,400), sh 395(10,200). Anal. Calcd. for $C_{56}H_{88}Li_2N_2P_4$: C, 72.55; H, 9.57; N, 3.02. Found: C, 73.21; H, 9.43; N, 3.14.

Synthesis of {(PNP)Cu}$_2$, 3.2: A solution of {**[3.1]Li**}$_2$ (1.0 g, 2.16 mmol) in diethyl ether (20 mL) was added to a slurry of CuBr·S(CH_3)$_2$ (0.466 g, 2.27 mmol) in ether (30 mL) and stirred for 12 h. The solvent was removed in vacuo and the resultant yellow solids were dissolved in petroleum ether (50 ml) and filtered to remove insoluble materials. Removal of petroleum ether and drying the yellow solids in vacuo afforded analytically pure material (1.04 g, 92%). Crystals suitable for X-ray diffraction were obtained both by slow-evaporation of a petroleum ether solution of **3.2**.

^{1}H NMR(499.9 MHz, CD_2Cl_2): δ 7.20 (m, 4H), 6.93 (m, 4H), 6.71 (br d, 4H), 6.61 (t, 4H), 1.806 (m, 4H), 1.58 (m, 8H), 1.39 (m, 8H), 1.29 (m, 4H), 0.99 (d, 12H), 0.73 (d, 12H), 0.70 (d, 12H), 0.60 (d, 12H). $^{13}C\{^{1}H\}$ NMR(125.7 MHz, CD_2Cl_2): δ 169.4, 131.8, 130.5, 128.7, 125.2, 117.8, 40.2, 36.4, 26.3, 26.2, 26.0, 25.7, 25.4, 25.1. $^{31}P\{^{1}H\}$ NMR (121.5MHz, C_6D_6): δ -33.9. UV-vis (cyclohexane, nm($M^{-1}cm^{-1}$)): 298(19,300), 314(19,900), 352(41,000), sh 387(14,300), 425(5100), sh 454(3400). Anal. calcd. for $C_{56}H_{88}Cu_2N_2P_4$: C, 64.65; H, 8.53; N, 2.69. Found: C, 64.54; H, 8.25; N, 2.62.

Quantum yield experiments. A volumetric solution of **3.2** (10 μM) in either cyclohexane (n = 1.426)[22] or tetrahydrofuran (n = 1.407) was prepared in a nitrogen-filled glove-box. Three cuvettes (1 cm path) were charged with this solution, sparged briefly with argon, and sealed with a greased ground-glass stopper. The absorption spectra were acquired both before and after fluorescence measurements to ensure the sample was not degrading. A solution of fluorescein in an aqueous 0.1 N NaOH solution was prepared and sparged with argon, the concentration was adjusted such that the optical density (OD) at 440 nm was the same as that of the individual solutions of **3.2**. Fluorescent measurements were performed with λ_{ex} = 440 nm at 298 K and corrected for detector response. The area under the curve of the emission spectrum was determined using standard trapezoidal integration methods. Quantum yields (Table III.1) were then calculated by the methods described by Demas and Crosby[23] using equation III.1.

$$Q = (Q_R)(I / I_R)(OD_R / OD)(n^2 / n_R^2) \qquad \text{(III.1)}$$

Q: quantum yield of the sample.

Q_R: quantum yield of fluorescein in aqueous 0.1 N NaOH solution (Q_R = 0.9).

I: integrated intensity of **3.2**.

I_R: integrated intensity of fluorescein sample.

OD_R: optical density of the fluorescein sample in absorption units.

OD: optical density of **3.2** in absorption units.

n: index of refraction of the solvent in which **3.2** was dissolved.

n_R: index of refraction of 0.1N NaOH solution (n_R = 1.3351), measured on a Bausch & Lomb refractometer.

Table III.2: Data for Quantum Yield Measurements.

Solution	OD (measured)	I (measured)	Q (calculated)
Fluorescein in 0.1N NaOH	0.0398	2.4725E+09	
10 μM **3.2** in cyclohexane	0.0352	1.5000E+09	0.70
10 μM **3.2** in cyclohexane	0.0369	1.5067E+09	0.67
10 μM **3.2** in cyclohexane	0.0408	1.6423E+09	0.67
		Average	**0.68**
		std. deviation	**0.02**
Solution	**OD (measured)**	**I (measured)**	**Q (calculated)**
Fluorescein in 0.1N NaOH	0.0119	6.5402E+08	
10 μM **3.2** in tetrahydrofuran	0.0174	6.6049E+08	0.69
10 μM **3.2** in tetrahydrofuran	0.0193	6.6209E+08	0.62
10 μM **3.2** in tetrahydrofuran	0.0137	5.3344E+08	0.71
		Average	**0.67**
		std. deviation	**0.04**

Lifetime measurements. A solution of **3.2** (10 μM) in either cyclohexane or tetrahydrofuran was prepared in a nitrogen-filled glove-box. The cuvettes (1 cm path) were charged with this solution, sparged briefly with argon, and sealed with a greased ground-glass stopper. The absorption spectra were acquired both before and after the fluorescence measurements to ensure the sample was not degrading. Fluorescent measurements were performed with λ_{ex} =460, λ_{em}= 510 nm at 298 K. A 500 nm low-pass filter was placed in front of the PMT in order to eliminate noise due to scattered laser light. The emission decay was averaged over 50 laser pulses and fit to an exponential function from which k_{obs} was determined (see Table III.3).

Table III.3: Data for Excited State Lifetime Measurements.

Entry	Solution	k_{obs} (s^{-1})	Lifetime (1/ k_{obs}) (μs)
1	10 μM **3.2** in tetrahydrofuran	8.9683E+04	11.15
2	10 μM **3.2** in tetrahydrofuran	8.9656E+04	11.15
3	10 μM **3.2** in tetrahydrofuran	9.4984E+04	10.53
		average	**10.94**
		std. deviation	**0.4**
	$k_{radiative}$[a](average)	6.22E+04	
	$k_{non\text{-}radiative}$[b] (average)	2.93E+04	
Entry	**Solution**	k_{obs} (s^{-1})	**Lifetime (1/ k_{obs}) (μs)**
4	10 μM **3.2** in cyclohexane[c]	9.6675E+04	10.34
5	10 μM **3.2** in cyclohexane	9.9590E+04	10.04
		average	**10.19**
		std. deviation	**0.2**
	$k_{radiative}$[a] (average)	6.58E+04	
	$k_{non\text{-}radiative}$[b] (average)	3.24E+04	

(a) $k_{radiative}$ = (Quantum Yield)/(Lifetime); (b) $k_{non\text{-}radiative} = k_{obs} - k_{radiative}$ (c) indicates the representative fit shown below

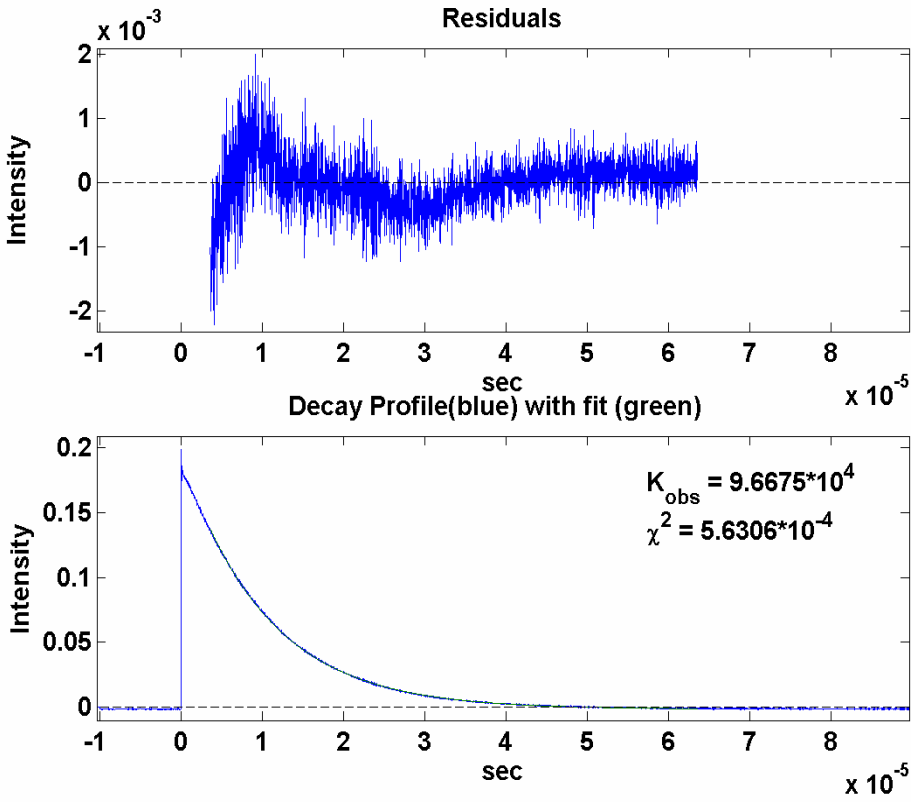

Graph III.2: Fit of the Excited State Decay with Residuals for Entry 4, Table III.3.

Time-resolved luminescent quenching experiments. A solution of **3.2** (20 μM) in tetrahydrofuran was prepared in a nitrogen-filled glove-box. Two cuvettes (1 cm path) were charged with 2 mL of this solution, sparged briefly with argon, and sealed with a rubber stopper. The initial emission decay of 2 in each cuvette was measured with λ_{ex} = 440 nm and λ_{em}= 500 nm prior to the introduction of the quencher. A solution of 2,6-dichloroquinone (DCQ) (10 mM) was then sequentially added to the cuvettes via syringe in volumes listed in Table III.4, and the emission decay was measured. The combined data from the two runs is plotted in Graph III.2, and a first order rate constant of 1.2×10^{10} $M^{-1}s^{-1}$ was determined for the emission quenching.

Table III.4: Time-resolved Emission Quenching Measurements.

Run 1		
μL of DCQ solution (total)	**μM of DCQ in sample**	**k_{obs} (s^{-1})**
0	0	2.1E+05
4	20	4.2E+05
20	99	1.3E+06
40	200	2.4E+06
80	380	4.7E+06
Run 2		
μL of DCQ solution (total)	**μM of DCQ in sample**	**k_{obs} (s^{-1})**
0	0	1.1E+05
10	50	9.7E+05
30	150	2.0E+06
50	240	3.2E+06
70	340	4.4E+06

III.D. References Cited

[1] (a) Elliott, C. M.; Pichot, F.; Bloom, C. J.; Rider, L. S. *J. Am. Chem. Soc.* **1998**, *120*, 6781. (b) Bargossi, C.; Fiorini, M. C.; Montalti, M.; Prodi, L.; Zaccheroni, N. *Coord. Chem. Rev.* **2000**, *208*, 17. (c) de Silva, A. P.; Fox, D. B.; Huxley, A. J. M.; Moody, T. S. *Coord. Chem. Rev*. **2000**, *205*, 41. (d) Drummond, T. G.; Hill, M. G.; Barton, J. K. *Nat. Biotech.* **2003**, *21*, 1192. (e) Sutin, N.; Creutz, C. *Pure & Appl.Chem.* **1980**, *52*, 2717.

[2] Ford, P. C.; Cariati, E.; Bourassa, J. *Chem Rev.* **1999**, *99*, 3625.

[3] McMillin, D. R.; McNett, K. M. *Chem*. *Rev.* **1998**, *98*, 1201.

[4] Cuttell, D. G.; Kuang, S.-M.; Fanwick, P. E. McMillin, D. R.; Walton, R. A. *J. Am. Chem. Soc.* **2002**, *124*, 6.

[5] Harkins, S. B.; Peters, J. C. *J. Am. Chem. Soc.* **2004**, *126*, 2885.

[6] Liang, L.-C.; Lin, J.-M.; Hung, C.-H. *Organometallics* **2003**, *15*, 3007.

[7] (a) Fryzuk, M. D.; MacNeil, P. A.; Rettig, S. J.; Secco, A. S.; Trotter, J. *Organometallics* **1982**, *1*, 918. (b) Fryzuk, M. D.; Leznoff, D. B.; Thompson, R. C.; Rettig, S. J. *J. Am. Chem. Soc.* **1998**, *120*, 10126.

[8] (a) Ozerov, O. V.; Guo, C.; Papkov, V. A.; Foxman, B. M. *J. Am. Chem. Soc.* **2004**, *126*, 4792. (b) Ozeroz, O. V.; Pink, M.; Watson, L. A.; Caulton, K. G.; *J. Am. Chem. Soc.* **2004**, *126*, 2105.

[9] Eriksson, H.; Håkansson, M. *Organometallics* **1997**, *16*, 4243.

[10] Low current signal is also evident at ~ -235 mV.

[11] Bill, E.; Müller, J.; Weyhermüller, T.; Wiegardt, K. *Inorg. Chem.* **1999**, *38*, 5792.

[12] Synthetic studies are underway to isolate and more thoroughly characterize the mono- and dicationic forms of the $\{(PNP)Cu\}_2^{n+}$ (n = 0, 1, 2) system.

[13] Luminescence measurements were collected in the Beckman Institute Laser Resource Center at the California Institute of Technology by previously published methods. Wenger, O. S.; Henling, L. M.; Day, M. W.; Winkler, J. R.; Gray, H. B. *Inorg. Chem.* **2004** , *43*, 2043.

[14] Demas, J. N.; Crosby, G. A. *J. Phys. Chem.* **1971**, *75*, 991.

[15] Maruyama, M.; Kaizu, Y. *J. Phys. Chem.* **1995**, *99*, 6152.

[16] Brown, I. D.; Dunitz, J. D. *Acta Crystallogr.* **1961**, *14*, 480.

[17] (a) Harvey, P. D. *Inorg. Chem.* **1995**, *34*, 2019. (b) Balzani, V.; Juris, A.; Venturi, M.; Campagna, S.; Serroni, S. *Chem. Rev.* **1996**, *96*, 759.

[18] Geometry optimization and electronic structure calculation (JAGUAR 5.0, B3LYP/LACVP**) were performed on the complete structure of the cation of **3** assuming a doublet ground-state (no symmetry constraints applied; crystallographic coordinates of **3** were used as the HF initial guess). Jaguar 5.0, Schrodinger, LLC, Portland, Oregon, 2002.

[19] Roundhill, D. M. In *Photochemistry and Photophysics of Metal Complexes*; Fackler, J. P., Jr.; Modern Inorganic Chemistry; Plenum Press: New York, NY, 1994; p. 49-55 and 165-210.

[20] (a) Heyduk, A, F.; Nocera, D. G. *Science* **2001**, *293*, 1639. (b) Gray, H. B.; Maverick, H. W. *Science* **1981**, *214*, 1201.

[21] Chávez, I.; et al. *J. Organomet. Chem*. **2000**, *601*, 126.

[22] Lide, D. R., Ed. *CRC Handbook of Chemistry and Physics, 77th Edition*; CRC Press: New York, NY, 1996.

[23] Demas, J. N.; Crosby, G. A. *J. Phys. Chem.* **1971**, *75*, 991